



Universidade do Porto

FEUP Faculdade de
Engenharia

INTEGRATED MASTER IN BIOENGINEERING

Resveratrol Loaded Lipid Nanoparticles for Brain Targeted Delivery

Joana Sofia Fontes de Queiroz

Dissertation presented according to the requirements for the degree in
**INTEGRATED MASTER IN BIOENGINEERING – SPECIALIZATION IN MOLECULAR
BIOTECHNOLOGY**

President of the Jury: Prof. Doutor Alexandre Tiedtke Quintanilha
(Full Professor of the Abel Salazar Biomedical Sciences Institute of University of Porto)

Supervisor: Prof. Doutora Maria de La Salette de Freitas Hipólito Reis Dias Rodrigues
(Associated Professor of the Faculty of Pharmacy of University of Porto)

Oporto, July 2013

Acknowledgements

For me this project was a challenge that turned out to be very rewarding and enriching. Feel that all the work was worth it is very gratifying. But I want to thank some people without whom it would not be possible to implement this project.

I'm very grateful to my supervisor, Dra. Sallete Reis, firsts for giving me the opportunity to join in her team providing me all the means to develop this project and for her always constructive critique and encouragement, which helped me to conceptualize and accomplish my Dissertation.

I also wanted to give a special thanks to Ana RuteNeves (Nini) who was tireless throughout the development of my project, I want to thank all the availability, support, comfort and aid given since without her will be impossible to get where I am. Thanks for all from the bottom of my heart.

I would also like to say thanks to everyone in the Departamento de Química-Física da Faculdade de Farmácia da Universidade do Porto laboratory for making me feel so welcome, give me all the support scientific and moral and especially the good environment which provides a greater motivation and commitment of the people.

My sincere gratitude to the constant support, encouragement and unconditional love of my family and friends.

The number of people giving me their support has been crucial along the way and I'm very grateful to each and every person support that contributed to the accomplishment of this dissertation.

Contents

Acknowledgements	2
List of figures	5
List of tables	8
List of abbreviations	9
Abstrac	11
Resumo	113
Organization of the dissertation	15
Motivation and Objectives	16
General and Specific objectives	16
State-of-the-art	18
Resveratrol	18
Nanoparticles for resveratrol delivery	23
Solid Lipid Nanoparticles (SLNs).....	23
Directing to Blood-brain barrier ...	27
Materials and Methods	30
Materials.....	30
Preparation of SLNs.....	31
Functionalization of Nanoparticles.....	32
Morphology determination.....	35
Particle Size measurements.....	36
Zeta Potential measurements.....	37
Resveratrol Entrapment Efficiency	38
In vitro resveratrol release studies.....	38
Lyophilization.....	39
FTIR.....	40

Fluorometric assay.....	41
Statistical analysis.....	41
Results and Discussion	42
Optimizing parameters of SLNs production method	42
Characterization of non-functionalized SLNs	44
Morphology.....	44
Resveratrol EE.....	45
Particle size measurements.....	46
Zeta Potential measurements.....	47
Release studies.....	48
Stability study.....	49
SLNs Functionalized with ApoE.....	52
Strategy I: SLNs with DSPE-PEG-ApoE.....	52
Strategy II: SLNs with Palmitate-ApoE.....	55
Release study with functionalized nanoparticles.....	57
Stability study of functionalized nanoparticles.....	58
FTIR.....	60
Fluorometric Assay.....	62
Conclusion.....	64
Future work	66
Bibliography	67
Annex.....	72

List of figures

Figure Page

1. Chemical structures of resveratrol isomers.	18
2. Illustrative structure of SLNs.	24
3. Preparation method of SLNs.	31
4. Activation of avidin with EDC.	32
5. Peptide Bond between avidin and DSPE nanoparticles to form nanoparticles (NP's) conjugated with avidin.	33
6. Binding of avidin to palmitate performed at 37°C during 3 hours to form avidinpalmitate.	34
7. Mechanism of conjugation between biotin and Apo E.	34
8. Scattering effect.	37
9. FTIR equipment.	40
10. Molecular structure of fluorescein biotin.	41
11. TEM image of SLN Placebo.	44
12. TEM image of SLN RSV.	45
13. <i>In vitro</i> resveratrol release profiles from resveratrol-loaded lipid nanoparticles with different concentrations of resveratrol in SBF.	48
14. Effect of time of storage (at 10°C) on particle size for solid lipid nanoparticles at different concentrations of resveratrol.	50
15. Effect of time of storage (at 10°C) on zeta potential for solid lipid nanoparticles at different concentrations of resveratrol.	51
16. Effect of time of storage (at 10°C) on resveratrol entrapment	

Efficiency for solid lipid nanoparticles at different concentrations of resveratrol.	52
17. TEM image of SLN-DSPE-ApoE placebo.	53
18. TEM image of SLN-DSPE-ApoE RSV.	53
19. TEM image of SLN-Palmitate-ApoE Placebo.	55
20. TEM image of SLN-Palmitate-ApoE RSV.	55
21. <i>In vitro</i> resveratrol release profiles from non-functionalized SLNs and functionalized SLNs, in SBF.	57
22. Effect of time of storage (at 10°C) on particle size of ApoE functionalized SLNs.	58
23. Effect of time of storage (at 10°C) on zeta potential of ApoE functionalized SLNs.	59
24. Effect of time of storage (at 10°C) on entrapment efficiency of ApoE functionalized SLNs.	60
25. Infrared spectrum obtained by FTIR for SLNs with no functionalization, SLNs with avidin palmitate and avidin palmitate as a reference to compare with the functionalized samples.	60
26. Infrared spectrum obtained by FTIR for SLNs with no functionalization, SLNs with ApoE and biotinylated ApoE as a reference to compare with the functionalized samples.	61
27. Biotin Structure.	61
28. Infrared spectrum obtained by FTIR of SLNs with no functionalization, SLNs with ApoE and biotinylated ApoE as a reference to compare with the functionalized samples.	62

29. Fluorometric assay using fluorescein biotin to comprove the presence of ApoE in the samples functionalized using palmitate.	62
30. Fluorometric assay using fluorescein biotin to comprove the presence of ApoE in the samples functionalized using DSPE.	63
31. Microscope image of hCMEC/D3 cell line.	66
A1. Pictures of the SLNs synthesized during the optimization process.	72

List of tables

TablePage

I.	Times of Ultra-Turrax and sonication, sonication intensity and composition of the surfactant (polysorbate 80) tested for the different SLNs formulations.	42
II.	Size and PI for the different SLNs synthesized with different conditions.	43
III.	Characterization of resveratrol-loaded SLNs.	46
IV.	Characterization of SLNs with ApoE using DSPE.	54
V.	Characterization of SLNs with ApoE using palmitate.	56
AI.	Visual characterization of SLNs developed during the optimization process.	73

List of abbreviations

ABC	ATP-binding Cassette
ApoE	ApolipoproteinE
ApoE2	Apolipoprotein E2
ApoE3	Apolipoprotein E3
ApoE4	Apolipoprotein E4
BBB	Blood-Brain Barrier
CNS	Central Nervous System
DLS	Dynamic Light Scattering
DPSE	1,2-Distearoyl-sn-glycero-3-phosphoethanolamine
EDC	1-Ethyl-3-(3-dimethylaminopropyl) carbodiimide
EE	Entrapment Efficiency
ELS	Electrophoretic light scattering
FOXO	Forkhead transcription factor
FTIR	Fourier transform infrared spectroscopy
LDL	Low Density Lipoprotein
LRP	Low-density Lipoprotein Receptor
LRP1	Low-density Lipoprotein Receptor 1
LRP2	Low-density Lipoprotein Receptor 2
MPS	Mononuclear phagocyte system
MPTP	1-methyl-4-phenyl-1,2,3,6-tetrahydropyridine
NO	Nitric Oxide
NPs	Nanoparticles
P-gp	P-glycoprotein

PI	Polydispersity index
SBF	Simulated Body Fluid
SIRT	Human sirtuin
SLNs	Solid lipid nanoparticles
TEM	Transmission Electronic Microscopy

Abstract

Resveratrol is a polyphenolic compound produced by a wide variety of plants. This compound has interesting functions namely as antioxidant, anti-inflammatory, anticarcinogenic, cell cycle inhibitor, anti-aging, cardioprotector, neuroprotector, obesity and diabetes preventive. The purpose of this study is to take advantage of the beneficial effects of resveratrol as a neuroprotector reducing the risk of neurodegenerative disorders, especially Alzheimer's disease and Parkinson's disease and reducing the risk of brain cancer due to its antioxidant, anti-inflammatory and anticarcinogenic activity. However the blood-brain barrier represents a considerable obstacle to brain entry of the majority of drugs and thus severely restricts the therapy of many serious central nervous system diseases.

Furthermore, the pharmacokinetic properties of resveratrol are not favorable to its free administration, since the compound has poor bioavailability, low water solubility, and is chemically unstable. Therefore the aim is to develop a specific functionalized drug delivery system that protects resveratrol during its transit inside the organism until it reaches the target preserving its pharmacological properties and protecting from degradation and, at the same time, directing this drug to brain where it can exercise its neuroprotective effects.

Solid lipid nanoparticles (SLNs) loaded with resveratrol were produced and successfully functionalized with ApoE since apolipoprotein E is sufficient to mediate the transport of NPs into the brain. The formulations were completely characterized to evaluate the quality of the developed resveratrol-loaded nanoparticles for targeted brain drug delivery.

TEM images revealed that these formulations produce two populations of nanoparticles, one that stands out clearly and is characterized by having a size well below (<150 nm), and other, less pronounced, but with a greater diameter (~ 200 nm). An average resveratrol entrapment efficiency over 90% was obtained for both SLNs with ApoE using DSPE or palmitate. Dynamic light scattering measurements gave

a Z-average of ~ 170 nm in the case of DSPE and a Z-average of ~ 200 nm in the case of palmitate with a PI of <0.2 , and a reasonable negative zeta potential of around -13 mV. These characteristics remained unchanged for at least 1 month. The release studies showed that the system is capable of providing a controlled and prolonged release of resveratrol with small losses of drug until it reaches its target (the brain).

Functionalization of SLNs with ApoE was clearly demonstrated through fluorometric assays and evaluating the infrared spectra (using FTIR) for both types of functionalization performed.

The results suggest that the functionalization of SLNs with ApoE resulted in dynamic stable systems capable of being used as controlled-release models for targeting brain delivery of resveratrol. Both functionalized nanodelivery systems (DSPE mediated and palmitate mediated) can be considered suitable carriers for resveratrol, conferring protection to this drug, targeting to the brain and allowing a controlled release after achieve the therapeutic target.

Resumo

O resveratrol é um composto polifenólico produzido por uma grande variedade de plantas. Este composto apresenta funções bastante atraentes do ponto de vista científico, nomeadamente como antioxidante, anti-inflamatório, anticarcinogénico, inibidor do ciclo celular, anti envelhecimento, cardioprotetor, neuroprotetor, prevenção de obesidade e diabetes e possível extensão do tempo de vida. O objectivo deste projeto é tirar partido dos efeitos benéficos de resveratrol como neuroprotetor, reduzindo o risco de doenças neurodegenerativas, especialmente da doença de Alzheimer e doença de Parkinson, e reduzindo o risco de cancro do cérebro, devido às suas propriedades antioxidantes, anti-inflamatória e actividade anticarcinogénica. Contudo, a barreira hematoencefálica representa um obstáculo considerável à entrada no cérebro da maioria dos medicamentos e, assim, restringe severamente o tratamento de muitas doenças graves do sistema nervoso central.

Para além disso, as propriedades farmacocinéticas de resveratrol não são favoráveis à sua administração livre, uma vez que o composto apresenta uma fraca biodisponibilidade, baixa solubilidade em água e é quimicamente instável. Por conseguinte, o objectivo é desenvolver um sistema de entrega do fármaco funcionalizado que proteja o resveratrol durante o seu trajeto no interior do organismo até atingir o alvo, preservando as suas propriedades farmacológicas e protegendo-o da degradação e, ao mesmo tempo, dirigindo-o para o cérebro, onde poderá exercer os seus efeitos neuroprotetores.

Nanopartículas sólidas lipídicas (SLNs) com resveratrol foram produzidas e funcionalizadas com sucesso com a ApoE3, uma vez que a apolipoproteína E3 é suficiente para mediar o transporte de nanopartículas para o cérebro. As formulações foram completamente caracterizadas para avaliar a qualidade das nanopartículas contendo resveratrol para a entrega do fármaco no cérebro.

As imagens de TEM revelaram que estas formulações produziram duas populações de nanopartículas, uma que se destaca de forma clara e é caracterizada por ter um tamanho bastante inferior ($< 150\text{nm}$), e outra, menos pronunciada, mas

com um diâmetro maior (~200 nm). Uma eficiência de encapsulação de resveratrol superior a 90% foi obtida para os dois tipos de SLNs funcionalizadas com ApoE, usando DSPE ou palmitato. As medições de dispersão dinâmica de luz revelaram um tamanho médio de 170 nm no caso da funcionalização com DSPE, e de aproximadamente 200 nm no caso da funcionalização com palmitato, com um índice de polidispersão inferior a 0,2 e um potencial zeta razoavelmente negativo de cerca de -13 mV. Estas características permaneceram inalteradas durante pelo menos 1 mês de armazenamento. Os estudos de liberação mostraram que o sistema é capaz de proporcionar uma liberação controlada e prolongada de resveratrol, com pequenas perdas de fármaco até este atingir o seu alvo (o cérebro).

A funcionalização das SLNs com a ApoE foi claramente demonstrada para ambos os tipos de funcionalização desenvolvidos, através de ensaios fluorimétricos e avaliando o espectro de infravermelhos das amostras (usando FTIR).

Os resultados obtidos sugerem que a funcionalização das SLNs com ApoE resultou em sistemas estáveis capazes de serem usadas como modelos de liberação controlada de resveratrol no cérebro. Ambos os nanossistemas funcionalizados (usando DSPE ou usando palmitato para adicionar a ApoE ao sistema) são inovadores e podem ser considerados como adequados para o transporte de resveratrol, conferindo protecção ao fármaco, direccionando-o para o cérebro e permitindo uma liberação controlada após atingir o alvo terapêutico.

Organization of the dissertation

The dissertation is constituted by:

1. **Motivation and Objectives** where basic necessary information provides a framework to the research topic, with an explanation why the subject was chosen for study, the description of the main and secondary goals of the dissertation, and the general organization of this dissertation;
2. **State-of-the-art** where a relevant literature review is made on the subject of this work which includes: properties of resveratrol, problems in resveratrol pharmacokinetics, the potential of SLNs in brain drug delivery, the challenges of crossing blood-brain barrier (BBB) and namely the strategies of SLNs functionalization;
3. **Materials and Methods** where is mentioned the list of materials used and their sources and all the methodologies used in the course of this work as well as its relevance to the work;
4. **Results and Discussion** where the results are presented and accompanied by the respect discussion in the context of the literature review;
5. **Conclusions** where it is summarized in some way the advantages and utility of the formulations developed. It is also presented the main conclusions based on the results obtained and the initial goals of this dissertation with a personal appreciation of the work developed.
6. **Future research** is the last section where are described suggestions of possible future work that can be important for the current project.

This dissertation has also an **annex** where all the supplementary results are included.

Motivation and Objectives

Resveratrol is a natural polyphenolic phytochemical compound with a variety of bioactivities associated with prevention of diseases and health promotion. Recent works have proved that this compound has beneficial effects on neurological disorders such as neurodegenerative diseases, specially on their prevention. However, when resveratrol is administered in its free form it presents a poor bioavailability, a low solubility and is rapidly metabolized losing its therapeutic activity. Considering this, the amount of resveratrol that truly reach the brain would be almost residual.

General and Specific objectives

In this context, the aim of the current work is the development of resveratrol loaded lipid nanoparticles for enhanced brain targeted drug delivery, taking advantage of the neuroprotective effects of resveratrol. SLNs will be employed in this study since they are known to be a promising drug delivery system to enhance brain uptake of many drugs and can easily be functionalized. The goal is to functionalize SLNs with apolipoprotein E (ApoE) in order to direct it to the brain because ApoE-modified nanoparticles could interact with apolipoprotein receptors (e.g. LDL receptor-related protein) at the BBB resulting in their endocytotic uptake into endothelium and transcytosis into the brain.

Therefore, in order to accomplish the main objective of developing a valid functionalized nanocarrier system to encapsulate resveratrol, several other specific goals had to be established and achieved:

- Optimization of nanoparticles to achieve an average size of 150 nm (the composition of particles and parameters of the modified hot homogenization technique for the production of SLNs had to be optimized, e.g. the amount of surfactant (polysorbate 80), the time of stirring, the time of sonication and the sonication intensity);
- Functionalization of nanoparticles for targeting to the brain (ApoE as target to LDL receptor in BBB);

- Nanoparticles produced (with and without functionalization) were characterized by the determination of: (i) particle size measurements i.e., determination of the average hydrodynamic diameter and polydispersity index (PI) using dynamic light scattering (DLS); (ii) zeta potential measurements using electrophoretic light scattering (ELS); (iii) entrapment efficiency (EE) measured with UV-spectrophotometer; and (iv) morphology analyzed by transmission electron microscopy (TEM);
- Evaluation of the nanoparticles stability during 2 months for SLNs with no functionalization and 1 month for functionalized SLNs, allowing to infer about the nanoparticles shelf stability and the behavior of the nanoparticles during storage. The stability was verified over time by measuring the particles' size, PI, zeta potential and entrapment efficiency;
- To check and confirm the functionalization of the nanoparticles, we have performed fluorometric assays using a fluorescent probe and also infrared spectra of each sample in the Fourier transform infrared spectroscopy (FTIR) to verify the presence of specific functional groups characteristic of the functionalization;
- Controlled release studies in simulated body fluid (SBF) were also performed to predict the release pattern of resveratrol in the bloodstream for both SLNs (with and without functionalization).

State-of-the-art

Resveratrol

Resveratrol ($C_{14}H_{12}O_3$) is a natural polyphenolic antioxidant compound produced by a broad variety of plants and its structure is represented in figure 1.^[1] Apart from all other sources, resveratrol may be found in high concentrations in the skin of grapes and their seeds.^[2] This natural compound has been classified as a natural phytoalexin for being synthesized *de novo* by plants in response to injury, ozone exposure, UV irradiation and in response to fungal attack constituting a defense mechanism for the plant.^[3-8] Resveratrol exists in *cis* and *trans* isomeric forms (represented in figure 1) although the *trans*-isomer is believed to be the most abundant and biologically active form.^[9,11]

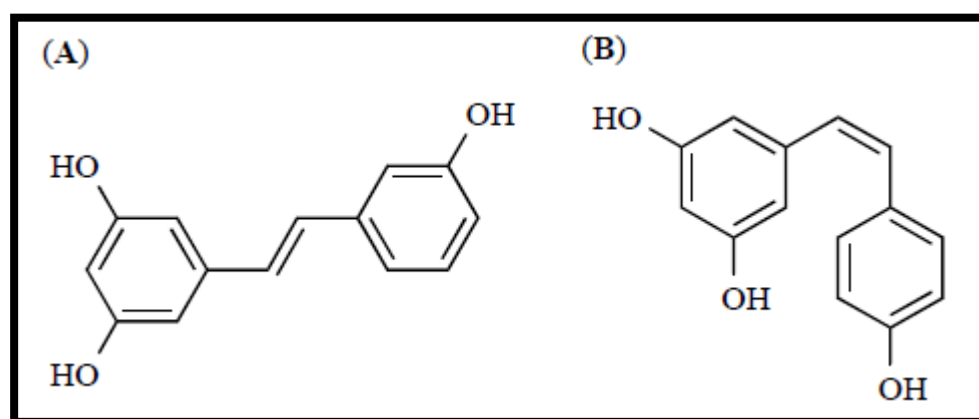


Figure 1 • Chemical structures of resveratrol isomers. (A) *trans*-resveratrol and (B) *cis*-resveratrol.

French Paradox

As mentioned before one of the richest natural sources of resveratrol is the dark grapes and consequently the wines that are produced from these grapes. Resveratrol became popular when the consumption of red wine was linked with the low incidence of cardiovascular diseases, a phenomenon commonly known as the *French Paradox*. It is believed that polyphenolic antioxidants offer protective effects for the cardiovascular system and in fact, certain populations of France, in spite of regular consumption of high fat diet and low exercise practice, appear to have less predisposition to heart diseases^[1,12]. Is very interesting the fact that despite a high

level of risk factors (such as cholesterol, diabetes, hypertension and a high uptake of saturated fat), French males display the lowest mortality rate from ischemic heart disease and cardiovascular diseases in Western industrialized nations (36% lower than the USA and 39% lower than the UK).^[13]

Thus, a mild-to-moderate wine drinking habit attenuates cardiovascular, cerebrovascular, and peripheral vascular risks due to the reduced platelet adhesion. It also attenuates the risk of a variety of cancers including pancreatic, gastric, and thyroid cancer, and slows down some neurodegenerative diseases like Alzheimer's disease and Parkinson's disease.^[10]

Among approximately 500 different antioxidants (including resveratrol, catechin, epicatechin and proanthocyanidins.), recent studies revealed that resveratrol and proanthocyanidins are the two most important polyphenolic antioxidants present in wine that attenuate various health problems by reducing myocardial ischemic reperfusion injury.^[14] In fact, resveratrol is the principal compound present in red wine that is responsible for *French Paradox*.

Intracellular Activity of Resveratrol

The interest of the scientific community in resveratrol has grown over the years due to its features and its wide biological and pharmacological activities at the cellular level which have been demonstrated.

This phytoalexin has **anticarcinogenic activity** because it was able to positively modulate a huge variety of intracellular signaling molecules involved in multi-stage carcinogenesis, inflammation, cell cycle, and apoptosis by scavenging of free radicals, suppression of cyclooxygenase activity, inhibition of cell proliferation, induction of apoptosis, and inhibition of enzymes, namely ribonucleotide reductase, DNA polymerases and protein kinase C. Associated with this anticarcinogenic activity come the potential of resveratrol as **antioxidant** by scavenging radicals like hydroxyl, superoxide, and others, protecting cell membranes against lipid peroxidation and avoiding DNA damage caused by the generation of reactive oxygen species (ROS).^[1] On the other hand resveratrol has shown to exhibit anticarcinogenic effects also due to

anti-inflammatory activity of this compound by blocking the expression of various components of pro-inflammatory signaling (such as iNOS, IFN- γ , pro-inflammatory cytokines and TNF- α), through the suppression of nuclear factor-KB (NF-KB) and the activator protein-1 (AP-1).^[1,11] Thereby, its anti-inflammatory and antioxidant activity jointly with the potential to induce cell cycle arrest and apoptosis are responsible for the chemopreventive effects of resveratrol.^[1]

As already mentioned resveratrol has **cardioprotective effects** associated with the *French Paradox*. Several mechanisms have been suggested to explain this cardioprotective effect of resveratrol which include, for example, the ability to inhibit the secretion of catecholamines that contribute to the increased risk of heart failures, atherosclerosis, coronary heart disease and hypertension; to modulate the production of NO from vascular endothelium which might control the inflammatory responses and prevent vascular damage (by inhibiting NF-KB that regulates iNOS expression in endothelial cells); and to inhibit eicosanoid synthesis from arachidonic acid that leads to the decrease of platelet aggregation.^[1] This anti-aggregating effect of resveratrol inhibit thrombus formation (atherosclerosis protection). In this case, as proved by Bertelli, *cis*-resveratrol was able to decrease collagen-induced platelet aggregation while *trans*-resveratrol at the same concentration showed a slightly lower activity.^[9]

Beyond the anticarcinogenic and cardioprotective effects, resveratrol has been shown to have **neuroprotective effects** in some neurological disorders, such as Alzheimer's disease, Parkinson's disease, Huntington's disease, brain ischemia, and epilepsy.^[1,21] Promising data within the use of resveratrol have been obtained by Saiko and his team, regarding the progressive neurodegenerative diseases such as Alzheimer, Huntington, and Parkinson. Because neurotoxicity is often related to mitochondrial dysfunction and may be ameliorated through the inclusion of metabolic modifiers and/or antioxidants, resveratrol may provide an alternative intervention approach that could prevent further damage and act at the level of prevention of brain diseases.^[17] Indeed moderate consumption of wine is associated with a lower incidence of Alzheimer's disease because wine is enriched in antioxidant compounds (like resveratrol) with potential to neuroprotective activities.^[18] In Alzheimer's disease,

resveratrol seems to lower the levels of secreted and intracellular A β peptides produced by different cell lines. In fact resveratrol does not inhibit A β production, because it has no effect on the A β -producing enzymes beta- and gamma-secretases, but promotes instead the intracellular degradation of A β peptides via a mechanism that involves the proteasome. Thus this natural compound has not only a preventive effect in Alzheimer's disease but also a therapeutic potential by its activity in proteasome-dependent anti-amyloidosis.^[18]

Relatively to Parkinson's disease, resveratrol exerts a neuroprotective effect on 6-hydroxydopamine-induced Parkinson rat model, and this protection is related to the reduced inflammatory reaction.^[19] Kwok-Tung Lu showed that resveratrol administration significantly protect mice from hydroxyl radical overloading, neuronal loss and motor coordination impairment induced by MPTP that is the most useful neurotoxin to induce Parkinsonism.^[20]

Recently, resveratrol was shown to **extend life span** in yeast through the activation of longevity gene SIRT1, which is also responsible for the longevity mediated by calorie restriction. In fact resveratrol mimics calorie restriction through the induction of expression of several longevity genes. These longevity genes include SIRT1s and FOXOs that act coordinately for the regulation of cell survival and longevity.^[10]

Apart from all the therapeutic properties already described, resveratrol has been shown to present **beneficial effects** also in **obesity and diabetes**, causing changes in gene expressions and in enzyme activities contributing to the prevention and treatment of insulin resistance, type II diabetes or dyslipidemia.^[1,16]

As we can see resveratrol may be useful in treating cardiovascular diseases, cancers, pain, inflammation, tissue injury, and in reducing the risk of neurodegenerative disorders, especially Alzheimer's disease and Parkinson's disease. The aim of this project is to take advantage of the neuroprotective effects of resveratrol to prevent the development of several neurological disorders that can have serious repercussions in terms of physical and mental health.

Problems in pharmacokinetic proprieties of resveratrol

Unfortunately, the pharmacokinetic properties of resveratrol are not as favorable when compared with its beneficial pharmacological activities in various disease models. This polyphenol has high oral absorption but is rapid and extensive metabolized resulting in only trace amounts of unchanged resveratrol in the systemic circulation. To give an idea, in humans, about 70 % of orally administered resveratrol (25 mg) is rapidly absorbed and metabolized (< 30 min).^[1] However we should also remember that there are some genetic aspects concerning ethnicity and genetic polymorphisms that affect the metabolism of compounds, existing variability in the time of drug metabolism. Extremely rapid sulfate conjugation in liver appears to be the rate-limiting step in resveratrol's bioavailability. Even though the systemic bioavailability of resveratrol is very low, the accumulation of resveratrol in epithelial cells along the aerodigestive tract and potentially active resveratrol metabolites may still produce cancerpreventive and other biological effects with much less efficiency.^[22]

The lipophilicity is one of the intrinsic properties of many drugs that influence the penetration of the drug molecule into the cell and consequently their ability to achieve the appropriate intracellular targets. Resveratrol has a partition coefficient of 3.1 (log P) being a hydrophobic drug. Substances very poorly soluble in water lead to low absorption and poor bioavailability in case of oral administration and may aggregate after intravenous administration leading to complications such as embolism or local toxicity.

In addition, the use of resveratrol is limited because it is a compound easily oxidizable and extremely photosensitive undergoing a transformation induced by light (UV) from the *trans* isomer to the *cis* isomer.

However the aim of this work was to take advantage of the neuroprotective effects of resveratrol and for this purpose the compound needs to reach the brain. If the compound was administered in its free form, little or no drug would reach the brain due to its low bioavailability, low water solubility, and its chemical instability which would lead to a rapid and extensive metabolization and excretion.^[2]

Therefore the development of specific functionalized drug delivery systems that protect resveratrol during its transit inside the organism until it reaches the target is extremely relevant to preserve its pharmacological properties protecting from degradation and at the same time directing this drug to brain where it can exercise its neuroprotective effects.

Nanoparticles for resveratrol delivery

The main advantages of using nanoparticles as drug delivery systems are the possibility of minimizing degradation of a drug after its administration and maximizing the therapeutic effects reducing unwanted side effects. With nanoparticles we can also increase the bioavailability of drugs and drive (by active or passive target) the drugs to the site of action increasing, in a specific or non-specific way, the concentration of a drug in the area of pathology. Moreover, the nanoparticle system has to be non-toxic (biodegradable, biocompatible, non bioaccumulative and non-immunogenic); have a small and controlled size; a large surface-volume ratio resulting in an increase of locals of interaction and locals to functionalize; a surface charged to prevent aggregation and increase the stability of the particles in solution; a high capacity to contain and carry a large amount of drug; and finally, like every product, must be economically viable and easily prepared.

Ideally nanoparticles for therapeutic usage should remain in circulation for an adequate time and be present at the site of action in adequate amounts to promote a controlled drug release and an efficient uptake by cells for improving the therapeutic efficacy.

Solid Lipid Nanoparticles (SLNs)

In the sequence of the work done by Neves et al.^[2], the vehicle for resveratrol transport developed was the SLNs which constitute an attractive colloidal resveratrol carrier system with very potential also for brain targeting.

SLNs consist of spherical solid lipid nanoparticles in the nanometer range, which are dispersed in water or in aqueous surfactant solution. SLNs are produced from solid lipids producing a solid matrix with few cavities at room and body temperatures (figure 2). They are made of one or more lipids with melting points higher than body temperature, so this carrier remains in solid state after administration.

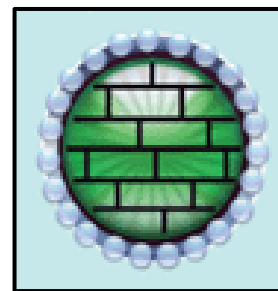


Figure 2 • Illustrative structure of SLNs.

These carriers have a hydrophobic core being specially adapted to the transport of hydrophobic drugs such as resveratrol. These controlled-release systems are suitable for transporting and protecting this important bioactive compound against degradation, increasing its physical stability and have a special ability to penetrate cell membranes, allowing the increased cellular uptake of compounds they are loaded with. ^[2,26]

SLNs are very promising since they combine a variety of advantages: ^[26]

- They are composed of biodegradable and biocompatible excipients ("GRAS" Lipids - generally recognized as safe, FDA);
- This is a water based technology, avoiding organic solvents that may be a focus of toxicity;
- These systems have a high physical stability;
- SLNs in a range of 120-200 nm are not taken up readily by the cells of mononuclear phagocyte system (MPS) and thus bypass liver and spleen filtration;
- It can be achieved a controlled release of the incorporated drug for up to several weeks;
- It is possible to functionalize the surface directing the drug to its site of action (maximizing therapeutic effects and minimizing side effects);
- Depending on the composition and preparation they may be quite stable over time;
- It can be achieved a high entrapment efficiency, depending on the drug lipophilicity properties;

- This is a delivery system economically more affordable than others because it is easy to scale-up due to its facility of preparation and reproducibility.

Therefore, SLNs have a lot of advantages as a system for drug delivery, namely for lipophilic compounds. However, our aim is that nanoparticles reach the brain, so we need to develop a specific target to BBB permeation. In the late 90s SLNs were proposed for brain drug targeting application even though the first proof of lipid particle transport across the BBB had already been provided.^[31]

Polymeric nanoparticles have been characterized as a good vehicle to deliver drugs into the brain although there are various problems associated with the use of these nanoparticles like residual contamination from production process (organic solvents), polymerization initiation, large polymer aggregates, toxic monomers and toxic degradation products, expensive production methods, lack of large scale production method and suitable sterilization method.^[26] Lipid-based nanocarriers hold strong promise to delivery of drugs to central nervous system (CNS) because these materials are biocompatible and biodegradable as already mentioned and because the lipophilic materials have the natural tendency to target through BBB.^[27] Several studies have been made to direct drugs to brain and there are other important features which makes the SLNs as appealing:

- Due to its lipid nature (lipophilic) SLNs have the natural tendency to cross the BBB;^[27]
- The SLNs appear suitable as a drug carrier system for potential intravenous use due to their very low cytotoxicity in vitro (SLNs cause less non-specific cell toxicity even compared to nanoparticles made of PLGA);^[28]
- P-gp efflux activity at brain endothelial cells can be bypassed using SLN formulations;^[29]

Thus, SLNs evidently hold strong promise for brain delivery of drugs and this was the carrier chosen for the development of a new brain targeted resveratrol delivery system.

For the preparation of SLNs it is necessary the use of one or more surfactants that stabilize the lipids in aqueous solution and allow the formation of spherical nanoparticles. However the type of surfactant used can be crucial to the success of the formulation since it determines the type of plasma proteins that will adsorb in the surface of the nanoparticles when they are administered. The composition of the protein layer is regarded as the decisive factor, for example immunoglobulin G is known to be a specific activator of the complement system promoting recognition and phagocytic uptake of particulate carriers by MPS, whereas albumin creates a more hydrophilic surface which was found to reduce the phagocytic uptake *in vivo*.^[32]

Other surfactants are active in producing protein binding by the nanoparticles, but only polysorbate 80 appears to preferentially adsorb Apo-E.^[30] In fact, polysorbate 80 coated polybutylcyanoacrylate nanoparticles showed a preferentially adsorbing ApoE on their surface when compared with other surfactants. Due to ApoE adsorbed on the surface, accumulation in the brain might occur because the LDL receptors are overexpressed in BBB and recognized the ApoE-modified nanoparticles. By this way polysorbate 80-stabilized SLNs might have the biggest potential of delivering drugs into the brain.^[32] In fact, nanoparticles coated with polysorbates have previously been shown to enable the transport of several drugs across the blood-brain barrier, which under normal circumstances is impermeable to these compounds.^[34]

However, Zensi has shown that maybe polysorbate 80 coating is not enough to induce the crossing over BBB because after 30 minutes of incubation with the nanoparticles only the nanoparticles with covalently bound ApoE were detected in brain capillary endothelial cells and neurons.^[25] No uptake into brain was detectable with nanoparticles with no ApoE despite having been reported.

Nevertheless the surfactant chosen for SLNs preparation was polysorbate 80 but to direct them to the brain it is necessary to add an active target so that our resveratrol delivery system can be effective.

Directing to Blood-brain barrier...

The BBB is a dynamic barrier protecting the brain against pathogenic organisms and unwanted substances. As a dynamic system the BBB is capable of responding to local changes and requirements and is able to be regulated via a number of mechanisms and cell types, in both physiology and pathological conditions.^[23] However BBB represents a considerable obstacle to brain entry of the majority of drugs and thus severely restricts the therapy of many serious CNS diseases including brain tumors, brainHIV, Alzheimer and other neurodegenerative diseases. Therefore, only small (MW<500 Da) and lipophilic molecules can penetrate into the vascular space. The two main reasons for the failure of the drug delivery to the brain are (i) the poor penetration of the drug molecule across the BBB that is related with the physicochemical characteristics of the therapeutic agent (like lipophilicity) and with the drug related factors at the BBB as concentration, the size, conformation, ionization, and others; (ii) the back transport of drugs from the brain to the blood that depend on the affinity for efflux mechanisms.^[26] There are several membrane transporters located in the barrier which mediate the molecules efflux from the CNS compartment back to the blood and most of these transporters belong to the superfamily of ATP-binding Cassette (ABC) membrane transporters. These are the most ubiquitously expressed and largest membrane-associated proteins superfamily known to date and they are involved in the translocation of both endogenous and exogenous substrates and metabolites against their concentration gradient. P-glycoprotein (P-gp) is probably the most studied and characterized ABC member and is known to be involved in the cellular extrusion of a broad range of drugs, having many kinds of substrates.^[27]

There are many strategies that have been proposed to improve the permeability of drugs across the BBB which include:^[27]

- Inhibition of ABC transporters, once it has been developed a number of chemical entities of blocking specific ABC-transporters (e.g. P-gp inhibitor);
- Hyper-osmotic opening of the BBB, once it is known that an hypertonic solution of mannitol or urea can shrink the capillary endothelial cells by inducing water efflux and subsequently opening the tight junctions network momentarily;
- Pharmacological disruption of BBB using cytotoxic agents especially alkylating agents (etoposide or cisplatin) that disrupt tight junctions and create openings between the endothelial cells;
- Drug modification approach creating pro-drugs with good lipophilicity that can cross the cell membrane of the endothelial cells by passive diffusion;
- Nanotechnology for drug delivery to the brain that with its flexibility and versatility can direct the drug to the target site and at the same time it is possible to reduce the dosing frequency using a carrier that releases the drug in a sustained manner.

This work intends to take advantage of nanotechnology developing solid lipid nanoparticles to increase the concentration of resveratrol in the brain which may exert its therapeutic effect. To cross this barrier extremely organized in the brain nanoparticles size must be a focal point. SLNs of a size below 200 nm have an increased blood circulation and thus an increase in the time for which the drug remains in contact with BBB and for the drug to be taken up by the brain.^[26]

Additionally the delivery process can be made more selective and efficient by tagging the nanocarrier surface with ligand molecules that match with a receptor type that is strongly and specifically expressed on the surface of the cells to be targeted. This is a highly regulated and energy-dependent process, but may allow the whole nanocarrier and the loaded drug to go through the BBB, even passing the drug efflux transporters.^[27] Especially ApoE appears to play a major role in the nanoparticle-mediated drug transport across the BBB, as mentioned before.^[33]

Following this, we propose directing our resveratrol loaded SLNs to LDL receptors in the brain by covalently bound ApoE to the SLNs surface.

LRP1 (low-density lipoprotein receptor related proteins 1) and LRP2 (low-density lipoprotein receptor related proteins 2) are multifunctional, multi-ligand scavenger and signaling receptors, widely expressed in several tissues, and together they can interact with a very diverse range of molecules and mediators including ApoE. This apolipoprotein plays an important role in the transport of lipoproteins into the brain via LDL receptors.^[32] It is believed that the lipoprotein ApoE bound on nanoparticles surfaces, followed by LDL receptor mediated endocytosis and transcytosis facilitate the uptake of nanoparticles by the brain.^[24]

It has already been shown that the use of nanoparticles attached ApoE enabled the delivery of drugs across the BBB. In their study, Zensi produced PEGylated albumin nanoparticles with covalently bonded ApoE that enhanced uptake and intracellular localization in mouse endothelial cells. Thus nanoparticles with covalently bound ApoE are able to be taken up into the cerebral endothelium by an endocytic mechanism followed by transcytosis into brain parenchyma.^[25] Wagner and his group studied the uptake mechanism of ApoE-modified nanoparticles and clearly demonstrated the participation of LDL receptor family members, especially LRP1, on the specific ApoE-mediated nanoparticle uptake on brain endothelial cells.

In Caucasian populations there are three common variants of ApoE: ApoE2, ApoE3 and ApoE4. ApoE3 is the most frequent one, followed by ApoE4 and ApoE2. Within the ApoE family, ApoE3 and ApoE4 showed a higher binding affinity to the LDL receptor when compared to the other because ApoE2 is defective in binding to lipoprotein receptors presenting, for example, a <5% LDL receptor binding when compared with ApoE3 binding. Michaelis et al. showed that ApoE3 alone is sufficient to mediate loperamide transport to the brain by the specific event of recognition and binding to LDL receptors. ApoE-coupled nanoparticles may mimic lipoprotein particles (like LDL) that are endocytosed into the BBB endothelium and transcytosed through the BBB endothelium into the brain.^[34,35] Therefore, SLNs coupled to ApoE3 would be sufficient to mediate the transport of resveratrol into the brain.

Materials and Methods

Materials

For the nanoparticles synthesis, *trans*-resveratrol (more than 99% pure) was purchased from Sigma-Aldrich (St Louis, MO, USA), the solid lipid cetylpalmitate was provided by Gattefossé (Nanterre, France) and polysorbate 80 (Tween® 80) was supplied by Merck (Darmstadt, Germany). For the preparation of pH 7.4 phosphate buffer solutions, potassium phosphate monobasic was obtained from Sigma-Aldrich and sodium hydroxide from Riedel-de Haën (Seelze, Germany).

For the nanoparticles functionalization, sodium deoxycholate, avidin, NHS-palmitate, EDC and ApoE3 were provided by Sigma-Aldrich (St Louis, MO, USA), DSPE-PEG-NH₂ was purchased from Avanti Polar Lipids (Alabaster, Alabama, USA), and the biotinylation reagent [EZ-Link Sulfo-NHS (N-hydroxysuccinimido)-Biotin], the Snakeskin 10kDaMWCO dialysis tube, and the Slide-A-Lyzer Dialysis Cassette (10 kDa MWCO) were supplied by Thermo Scientific (Waltham, Massachusetts, USA).

For fluorometric assays, the fluorescein biotin was obtained from Life Technologies (Van Allen Way, Carlsbad, USA).

In preparation of SBF for resveratrol release studies dipotassium phosphate [K₂HPO₄] was purchased from Sigma-Aldrich (St Louis, MO, USA); calcium chloride [CaCl₂], sodium sulfate [Na₂SO₄] and tris(hydroxymethyl)aminomethane [(CH₂OH)₃CNH₂] were supplied by Merck (Darmstadt, Germany); sodium chloride [NaCl], magnesium chloride [MgCl₂] and sodium bicarbonate [NaHCO₃] were obtained from Riedel-de Haën (Seelze, Germany); potassium chloride [KCl] was purchased from Scharlau Chemie S.A. (Sentmenat, Barcelona, España); and finally, hydrochloric acid [HCl] was supplied by Panreac Química (Castellar del Valles, Barcelona, España).

The water used in all experiments during this project was purified water by Ultra-pure water system (Milli-Q RG), and was obtained from a reverse osmosis process.

Preparation of SLNs

The method chosen for the preparation of the nanoparticles was a good compromise between the high shear homogenization to produce particles in the micrometer range and the ultrasound method to reduce the microparticles to the nanometer range, see figure 3.

The lipid phase, containing cetylpalmitate (solid lipid), the stabilizer polysorbate 80, and the lipophilic resveratrol to be encapsulated (0, 2, 5, 10, or 15 mg) was melted at 70°C, which was above the lipid's melting point. The molten lipid was then dispersed in phosphate buffer pH 7.4, at the same temperature by high-speed stirring in an Ultra-Turrax T25 (Janke and Kunkel IKA-Labortechnik, Staufen, Germany) followed by sonication using a Sonics and Materials Vibra-Cell™ CV18 (Newtown, CT, USA). The mechanical shearing forces produced by the high-speed stirring in the Ultra-Turrax T25 produced a “pre-emulsion” of the lipid melt and aqueous surfactant producing particles in the micrometer range, while the sonication reduced the microparticles sizes to the nanometer range.^[36]

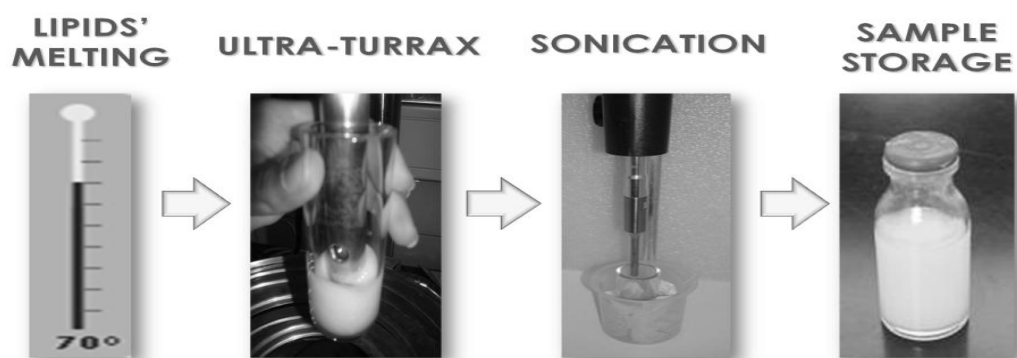


Figure 3●Preparation method of SLNs.

Some parameters of the high shear homogenization and ultrasound method technique for the lipid nanoparticles production were optimized in order to establish the best conditions for the production of formulation in terms of stability and optimization of average size (<200 nm). The content in solid lipid and surfactant was also tested in order to optimize the size and stability of the nanoparticles. After this previous optimization, the final parameters chosen were 120 seconds at 12,000 rpm in Ultra-Turrax, followed by 15 minutes of 80% intensity sonication and a percentage of

polysorbate 80 of 3%. All the components of the formulations were weighed in an analytical balance (Mettler Toledo AG285).

The formulations appeared white and milky and had low viscosity. The cooling of the nanoemulsions at room temperature allowed the crystallization of the lipid and subsequent formation of the lipid nanoparticles. To assess the stability of the formulations, they were stored at least for 1 month at 10 °C and the particle size, zeta potential and entrapment efficiency were measured periodically.

Functionalization of Nanoparticles

The challenging functionalization with ApoE takes advantage of the strongest known non-covalent interaction (K_d of 10^{-15} M) between a protein and ligand: the avidin-biotin complex. The bound formation between biotin and avidin is very rapid, and once formed, is unaffected by extremes of pH, temperature, organic solvents and other denaturing agents. Avidin is a tetrameric protein and has a very high affinity for up to four biotin molecules. Therefore, the functionalization of nanoparticles was performed by two different strategies: (i) using DSPE-PEG-avidin conjugated to the nanoparticles and (ii) using avidin palmitate conjugated to the nanoparticles. The avidin-conjugated nanoparticles then react with the previously biotinylated ApoE producing ApoE-functionalized SLNs.

Strategy I: Preparation of SLNs with DSPE-PEG-Avidin

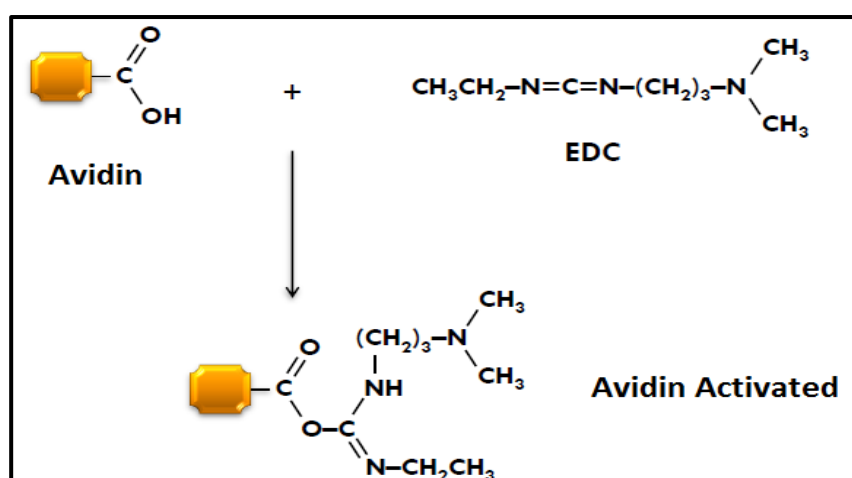


Figure 4 • Activation of avidin with EDC performed at room temperature for 30 minutes with stirring.

In this case, SLNs were prepared from the beginning as described above with the incorporation of DSPE-PEG-NH₂ in their composition. At the same time avidin solution was prepared at a concentration of 5 mg/ml by the dissolution of avidin in PBS. Avidin was later activated by incubation with EDC (in a ratio of 5:1, respectively) at room temperature for 30 minutes with stirring (figure 4).

After that, DSPE-containing nanoparticles (with a terminal amine group exposed on surface) were incubated at room temperature for 2 hours with the solution of avidin previously prepared and activated with EDC, giving rise to the nanoparticles conjugated with avidin (figure 5). The resulting nanoparticles were then dialysed in a snakeskin dialysis tubing MWCO 10 kDa against PBS, overnight at 37 °C, to remove the excess of avidin.

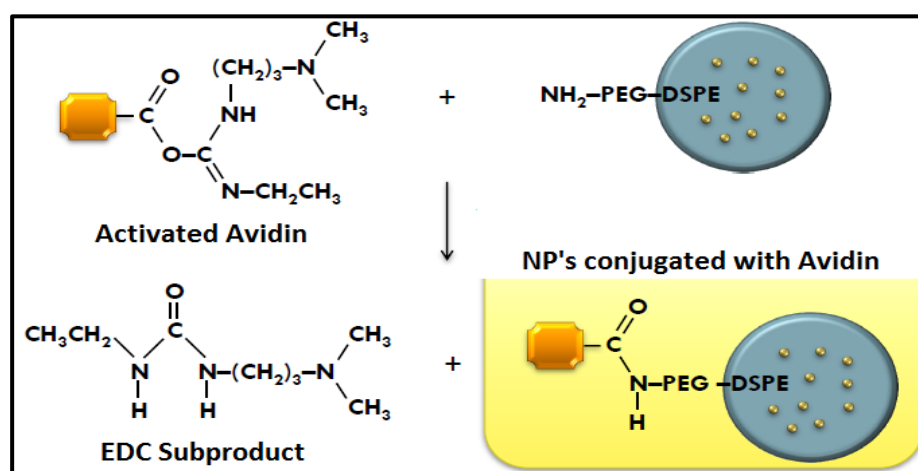


Figure 5 • Peptide bond formation between avidin and DSPE nanoparticles to form nanoparticles (NP's) conjugated with avidin. The reaction was performed at room temperature during 2 hours.

Strategy II: Preparation of SLNs with avidin palmitate

The avidin solution was firstly prepared at a concentration of 5 mg/ml by the dissolution of avidin in sodium deoxycholate (2%, pre-diluted in PBS). This solution was heated at 37°C with stirring until complete dissolution. NHS-palmitate was then added to the above solution and placed in an ultrasonic bath at 37°C until all palmitate flakes are dissolved. In order to promote the binding of avidin to palmitate, the solution formed was placed in a bath at 37°C for 3 hours (figure 6) and then dialysed in a dialysis tubing MWCO 10 kDa snakeskin against sodium deoxycholate (2%) at 37°C

overnight to remove excess avidin. Finally, the lipid nanoparticles were prepared as previously described but incorporating palmitate avidin in their constitution.

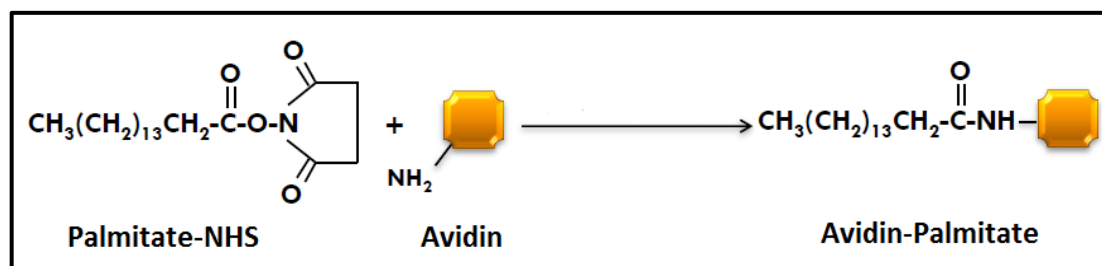


Figure 6● Binding of avidin to palmitate, performed at 37°C, during 3 hours to form avidin-palmitate.

Biotinylation of ApoE

ApoE solution was prepared by dissolving it in PBS to a final concentration of 0.2 mg/ml. Then, it was added the biotinylation reagent (sulfo-NHS-biotin) to the ApoE solution (in a ratio of 1:7, respectively), and it was incubated for 4 hours at 4°C, giving rise to biotinylated ApoE, see figure 7. Afterwards it was necessary to dialyse the solution of biotinylated ApoE to remove excess biotinylation reagent and ApoE that was not bound to the biotin. The dialysis was performed in a Slide-A-Lyser Dialysis Cassette (10 kDa MWCO) in 500 ml PBS, at 4°C for 8 hours, with medium change every two hours.

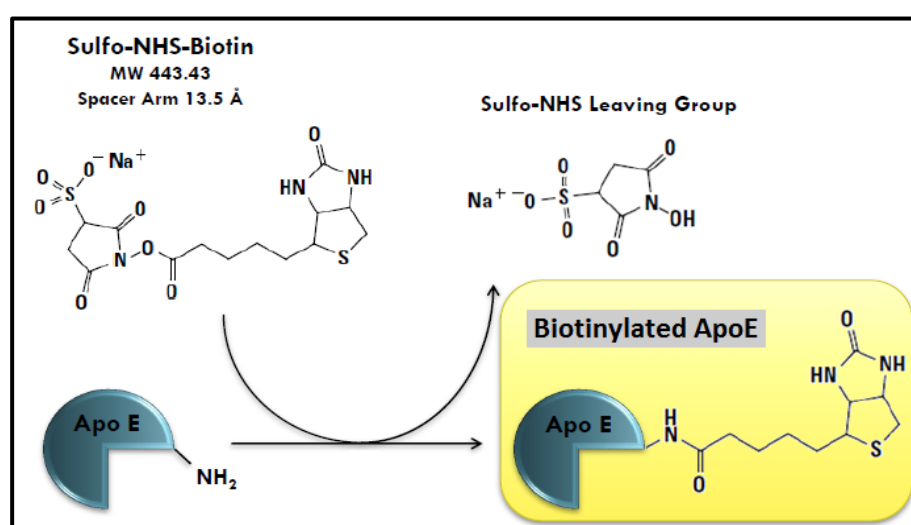


Figure 7● Mechanism of conjugation between biotin and ApoE.

Binding of biotinylated ApoE to SLNs conjugated with avidin

The binding of biotinylated ApoE to avidin conjugated SLNs was carried out by the spontaneous interaction of biotin and avidin, promoted by the simple contact between the two solution, for 30 minutes at room temperature. This strong interaction is the basis for the successful functionalization of nanoparticles with ApoE in order to direct them to the BBB and to promote the controlled release of resveratrol in CNS.

In order to check and confirm the functionalization of SLNs, we have performed fluorometric assays using a fluorescent probe (fluorescein biotin) and also infrared studies using FTIR, shown later in this chapter.

Morphology determination

To characterize the morphology of SLNs (with and without functionalization), the nanosystems were observed by TEM.

TEM utilizes energetic electrons to provide morphologic, compositional and crystallographic information of the samples. This equipment produces a high-resolution (maximum magnification of 1 nm), two-dimensional, black and white images resulting of the interactions that takes place between the prepared samples and the energetic electrons in the vacuum chamber. Air needs to be pumped out of the vacuum chamber to create a space where electrons are able to move.

The samples were mounted on 300 mesh form var copper grids, stained with uranyl acetate, and were examined using a Jeol JEM 1400 transmission electron microscope (Tokyo). Images were digitally recorded using a Gatan SC 1000 ORIUS CCD camera (Warrendale, PA, USA), and photomontages were performed using Adobe Photoshop CS software (Adobe Systems, San Jose, CA).

Particle Size measurements

Particle size analysis was performed by DLS, also known as photon correlation spectroscopy, using a particle size analyzer (Brookhaven Instruments, Holtsville, NY, USA).

This equipment is an important tool for measuring the size of nanoparticles in solution. DLS measures the light scattered from a laser that passes through a colloidal solution like shows figure 8. When a beam of light intersects a nanoparticle, part of the incident light is scattered. Moreover, nanoparticles in suspension are in constant motion (Brownian motions) due to the fact that small particles move randomly in solution as a consequence of the shocks between the fluid molecules and the particles in solution. Thus, this Brownian motions causes changes in scattered light intensity and by measuring the fluctuations of the scattered light intensity as a function of time, the DLS technique can give information about the mean hydrodynamic size (that includethehydrationspherethat surroundsthe particles), size distribution and PI of nanoparticles in suspension. PI is a measure of size variability, a unitless quantity derived from the commutations analysis and equivalent to the relative variance of the distribution that indicates the state of particle agglomeration. Thus, DLS does not directly measure the diameter of particles, but rather detects the fluctuations of light signals caused by the Brownian motion of the particles to calculate their sizes. ^[37]

As we can see in figure 8 larger particles will diffuse slower than smaller particles and the DLS instrument measures the time dependence of the scattered light to generate a correlation function that can be mathematically linked to a particle size and PI.

Prior to the measurements, all samples were diluted (1:200) using phosphate buffer pH 7.4 to yield a suitable scattering intensity. The average count rate was always between 100 and 500 kcps, showing that the dilution applied to the formulations was appropriate. DLS data were analyzed at 10°C and with a fixed light incidence angle of 90°. The mean hydrodynamic diameter (Z-average) and the PI were determined as a measure of the width of the particle size distribution. The Z-average and PI of the analyzed samples were obtained by calculating the average of ten runs. The measurements were always performed in triplicate.

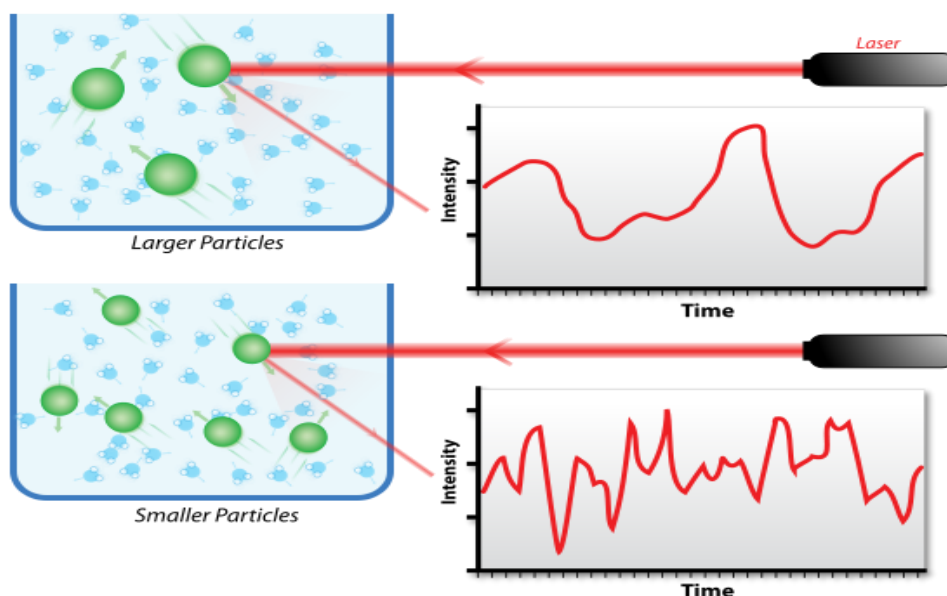


Figure 8●Scattering effect: when a beam of light falls on a nanoparticle the incident light is scattered depending on the particle size.

Zeta Potential measurements

The zeta potential was determined by measurement of the electrophoretic mobility using a zeta potential analyzer (Brookhaven Instruments, Holtsville, NY, USA).

The liquid layer surrounding the particle is formed by two parts: an inner region, called the Stern layer, where the ions are strongly bound; and an outer, more diffuse region where the ions are less firmly attached. Within the diffuse layer there is a notional boundary inside which the ions and particles form a stable entity. When a particle moves, ions within the boundary move with it, but any ions beyond the boundary do not travel with the particle. This boundary is called the surface of hydrodynamic shear and the potential that exists at this boundary is known as the zeta potential.^[38]

ELS is a technique to measure the zeta potential of a sample placed in a cell with electrodes. Then, an electric field is applied and the charged particles of the sample are attracted to the electrode of opposite charge. The laser passes through the sample, occurring electrophoresis and the frequency of light scattering caused by the particle is deflected. The frequency's deviation of the scattered light is proportional to electrophoretic mobility of the particles and therefore to the zeta potential.

The magnitude of the zeta potential gives an indication of the potential stability of the colloidal system. If all the particles have a very negative or very positive charge they will repel each other and therefore the dispersion has a good stability. If particles have a low zeta potential, there will be agglomeration and consequently instability in the dispersion.

Samples were diluted (1:200) with phosphate buffer (pH 7.4) and were analyzed at 10°C. The zeta potential of the analyzed samples was obtained by calculating the average of ten runs (each one with ten cycles). The measurements were performed always in triplicate.

Resveratrol Entrapment Efficiency (EE)

The EE of the drug was determined by calculating the difference between the total amount of resveratrol used to prepare the formulation and the amount of free resveratrol that was still present in the aqueous phase. The formulation samples were diluted in phosphate buffer (1:200) and transferred into Amicon® Ultra-4 Centrifugal Filter Devices (Millipore, Billerica, MA, USA). Centrifugation was performed using a Jouan BR4i multifunction centrifuge with a KeyWrite-D™ interface (Thermo Electron, Waltham, MA, USA) with a fixed 23°-angle rotor and 3300 *g* spin for 10 minutes. The untrapped resveratrol was present in the supernatant, which was stored in the centrifuge tube and quantified using a V-660 spectrophotometer (Jasco, Easton, MD, USA) at 200–600 nm. The EE was calculated as follows:

$$EE = \frac{\text{Total amount of resveratrol} - \text{Untrapped resveratrol}}{\text{Total amount of resveratrol}} \times 100$$

In vitro resveratrol release studies

The *in vitro* resveratrol release studies were performed using a cellulose dialysis bag diffusion technique (Cellu.Sep® T1 with a nominal molecular weight cut off of 3500 [Frilabo, Milheirós, Maia, Portugal]) filled with 2 mL of the sample (SLN 0, 2, 5, 10 and 15 mg of resveratrol).

We were interested in simulating the bloodstream conditions that would occur following intravenous administration to simulate the release of resveratrol from nanoparticles during the time that the nanoparticles take to reach their target (BBB).

Kokubo and his colleagues developed an acellular SBF that has inorganic ion concentrations nearly equal to those of human blood plasma and is buffered at pH 7.4 with 50 mM tris(hydroxy-methyl)aminomethane and 45 mM hydrochloric acid at 36.5°C.^[39,40]

For both nanoparticles (SLNs with and without functionalization) the samples were incubated for 28 hours in SBF at body temperature (37°C) while being stirred at 100 rpm. At regular intervals, aliquots were collected and replaced with the same volume of fresh medium of SBF to maintain the sink conditions. The resveratrol release was quantified using a V-660 spectrophotometer (Jasco, Easton, MD, USA) at 200–600 nm. The studies were conducted in triplicate and the cumulative percentage of released compound was determined by calculating the average, indicating the standard deviations (SDs).

Lyophilization

Samples of SLNs with and with no functionalization were lyophilized using an Advantage 2.0 benchtop freeze dryer (SP Scientific, Mearns Road Warminster, PA, USA). Lyophilization is a dehydration process that removes water and other solvents by the process of sublimation. This process was employed in order to use the samples in FTIR experiments because otherwise the water bands could mask the ones related to the sample itself. The lyophilization process started with freezing the samples processed at -60°C in vacuum for a period of 720 minutes for the water contained in the sample pass into a solid state and can sublime with the increase of temperature. Then, there was a drying of the samples at 20°C for 1200 minutes at 150 millitorr. Finally it took place a secondary drying at 25°C for 1200 minutes at 100 millitorr to increase the amount of sublimated water.

FTIR

To show and confirm the presence of ApoE in functionalized SLNs we have done infra-red spectra for each lyophilized samples using FTIR (see figure 9).

Infrared spectra result from transitions between quantized vibrational energy states. Molecular vibrations can range from the simple coupled motion of the two



Figure 9●FTIR equipment.

atoms of a diatomic molecule to the much more complex motion of each atom in a large polyfunctional molecule. The degrees of freedom give the number of ways that the atoms in a nonlinear molecule can vibrate and for many vibrational modes only a few atoms have large displacements and the rest of the molecule is almost stationary. The frequency of such modes is

characteristic of the specific functional groups in which the motion is centered. Therefore, the observation of spectral features in a certain region of the spectrum is often indicative of a specific chemical functional group in the molecule and by analyze the absorptions bands that is given in the infrared spectrum is possible to identify vibrational modes associated with a certain functional group. ^[41]

Besides the presence of functional groups, it is also possible to identify entire molecules because the infrared spectrum of a given molecule is unique and can be used to identify that molecule. ^[41]

As the corresponding band for water (OH vibrations) is sometimes too intense and wide for the hydrated sample it can hide or camouflage areas of the spectrum corresponding to important functional groups. As such, it often comes up the lyophilization of samples, for total removal of water, and are then plotted the infrared spectrumsof lyophilized samples that was what happened in this work. Thus 100 µl of the functionalized SLNs as well as reference SLNs (without functionalization) were lyophilized and infrared spectra plotted using a Frontier FT-IR Spectrometer from PerkinElmer (Santa Clara, California, USA).

Fluorometric assay

In addition to the infrared spectra, fluorometric assays were also performed to confirm the functionalization of the nanoparticles using a fluorescein biotin (in detail in figure 11) that can be used to quantify available biotin-binding sites through the strong quenching associated when this molecule binds to avidin. The fluorometric assays were performed in a Jasco FP-6500 spectrofluorometer (Easton, MD, USA).

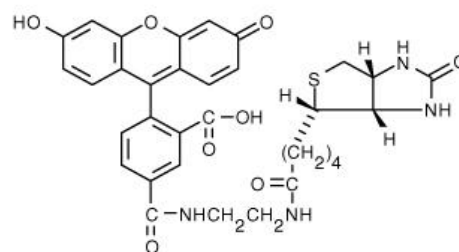


Figure 10●Molecular Structure of fluorescein biotin.

When biotinylated fluorescein binds to the avidin, this decreases the fluorescence due to quenching phenomenon. Thus, in the case of NPs conjugated with ApoE, the fluorescence signal must be greater because the avidin sites are occupied by ApoE and the fluorophore cannot bind, remaining free in solution. In the case of non-conjugation of ApoE to avidin-NPs, the fluorescence signal decreases due to the binding of biotin to avidin available in NPs.

Thus, a solution with probe was prepared at 200 mg/ml. The samples diluted in PBS (1:400) were incubated with biotinylated fluorescein during 30 minutes and then centrifuged in tubes with 100 nm filter at 4300 rpm until all the supernatant is collected (approximately 5 minutes). Samples supernatants were then gathered and its fluorescence read. The fluorescence (emission at $\lambda_{em}=518$ nm) of the free fluorescein biotin was detected by exciting the probe at a wavelength of $\lambda_{ex}=496$ nm (previously determined by tracing the excitation and emission spectra of this probe).

Statistical analysis

Statistical analyses were performed using SPSS software (v 18.0; IBM, Armonk, NY, USA). The measurements were repeated at least three times and data were expressed as mean \pm SD. Data were analyzed using one-way analysis of variance (one-way ANOVA), followed by Bonferroni, Tukey and Dunnett post-hoc tests. A *p* value of 0.05 was considered statistically significant.

Results and Discussion

Optimizing parameters of SLNs production method

The experimental part of this dissertation was initiated with the optimization of SLNs production at a level of size, not forgetting the stability over time.

Table I– Times of Ultra-Turrax and sonication, sonication intensity and composition of the surfactant (polysorbate 80) tested for different SLNs formulations.

	Ultra-Turrax (s)	Sonication		Polysorbate 80(%)
		Time(min)	Amplitude (%)	
SLN 1	30	5	80	3
SLN 2	120	5	80	3
SLN 3	120	15	80	3
SLN 4	120	15	90	3
SLN 5	120	30	80	3
SLN 6	120	60	80	3
SLN 7	120	90	80	3
SLN 8	120	30	90	3
SLN 9	120	60	90	3
SLN 10	120	15	100	3
SLN 11	120	30	100	3
SLN 12	120	15	60	3
SLN 13	120	5	60	3
SLN 14	120	30	60	3
SLN 15	120	5	50	3
SLN 16	120	15	50	3
SLN 17	120	30	50	3
SLN 18	120	5	60	5
SLN 19	120	5	50	5
SLN 20	120	5	70	3
SLN 21	120	5	60	2
SLN 22	120	10	50	3
SLN 23	120	10	60	3
SLN 24	120	5	50	4
SLN 25	120	5	55	3
SLN 26	120	5	50	2
SLN 27	60	5	50	2
SLN 28	60	5	60	2

The objective was to develop SLNs with an average size less than 200 nm to easily reach and cross their target (BBB). For this purpose, it has been tested some parameters of the high shear homogenization and ultrasound method technique in the SLN production as well as different compositions of the lipid nanoparticles (proportion of solid lipid and surfactant). Several combinations of time of stirring, time of sonication and sonication intensity combined with different compositions were tested to establish the best conditions for the production of formulations (Table I).

Table II–Size and PI for the different SLNs synthesized with different conditions.

As the goal in this step was to optimize the size of nanoparticles we have performed assays to measure the size of particles synthesized and the PI that gives us an idea of the heterogeneity of the sample. The results of this pre evaluation can be seen in Table II. A compromise between the adequate size, a low PI and also a good stability of the samples had to be considered for the final choice of the parameters to be used for SLNs synthesis.

In an attempt to preliminarily evaluate the temporal stability of the samples over time the SLNs with different compositions and preparation parameters were assessed approximately 3 weeks after they have been synthesized.

Thus, all formulations were characterized visually particularly in terms of milky

	Size(nm)	Polydispersityindex
SLN 1	158,0	0,098
SLN 2	195,0	0,005
SLN 3	176,0	0,219
SLN 4	168,0	0,108
SLN 5	144,4	0,110
SLN 6	150,3	0,170
SLN 7	146,4	0,144
SLN 8	193,4	0,145
SLN 9	203,6	0,157
SLN 10	168,3	0,159
SLN 11	179,2	0,141
SLN 12	151,8	0,139
SLN 13	125,0	0,176
SLN 14	135,0	0,088
SLN 15	99,0	0,314
SLN 16	138,5	0,124
SLN 17	142,9	0,100
SLN 18	129,1	0,178
SLN 19	144,3	0,164
SLN 20	155,3	0,137
SLN 21	116,5	0,145
SLN 22	101,2	0,294
SLN 23	137,6	0,080
SLN 24	117,0	0,211
SLN 25	87,4	0,309
SLN 26	80,8	0,323
SLN 27	145,1	0,103
SLN 28	103,3	0,146

appearance, presence of granules, air bubbles and foam, twophases and deposit formation (see table AI in annex).

Taking all this considerations into account, the final parameters chosen were 120 seconds of stirring in Ultra-Turrax, followed by 15 minutes of 80% intensity sonication, and a percentage of 3% of polysorbate 80 corresponding to the SLN 3.

Characterization of non-functionalized SLNs

Before the functionalization of SLNs, the formulations with different concentrations of resveratrol (0, 2, 5, 10, and 15 mg) were characterized according to their morphology, entrapment efficiency, average size, zeta potential and resveratrol release pattern.

Morphology

The morphology of the lipid nanoparticles (SLN Placebo) and resveratrol-loaded lipid nanoparticles (SLN RSV) was observed by TEM (figure 12 and figure 13, respectively). The images reveal that both SLNs were almost spherical and uniform in shape with smooth surfaces. As can be seen in figure 11 and 12 the mean

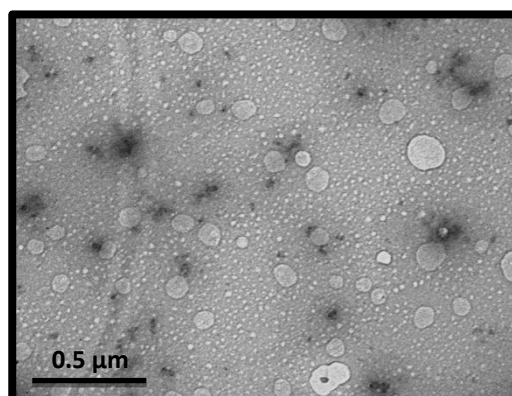


Figure 11 • TEM image of SLN Placebo.

diameter does not exceed the 200 nm. It is possible to see particles in the range of 100–200 nm or smaller and there was no visible aggregation of particles. TEM images revealed that these formulations produced two populations of nanoparticles, one most abundant with a smaller diameter, and other, less pronounced, with a larger

size. Undoubtedly, for both formulations (SLN Placebo and SLN RSV) the most frequent population of particles has a diameter lower than 150 nm.

Furthermore, the incorporation of resveratrol did not seem to cause morphological changes or crystal formation. Resveratrol-loaded lipid nanoparticles have a shape similar to placebo ones and the diameter seems to be in the same scale.

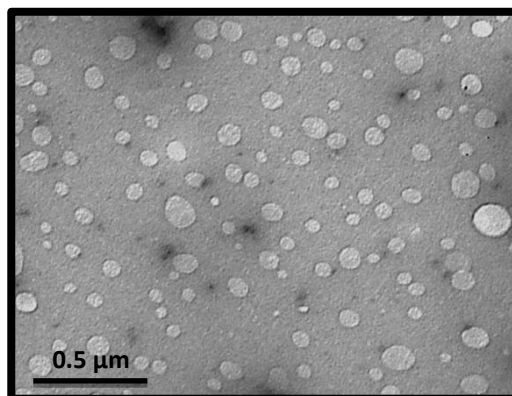


Figure 12 • TEM image of SLN RSV.

Resveratrol EE

Lipid nanoparticles are known to be suitable systems for drug incorporation that can prevent degradation and give protection to drug. The lipophilic nature of resveratrol that has an octanol/water partition coefficient ($\log P$) of 3.1 (predicted by the PubChem database) suggested its preferential partition into the lipid nanoparticles matrix instead of remaining in the aqueous media, which makes this type of nanoparticles quite advantageous for the incorporation of resveratrol.

The EE of each SLN formulation with a different resveratrol concentration is shown in Table III. The percentage of encapsulation of SLNs with resveratrol was found to be satisfactorily high, with an average EE of about 80%. With the increasing concentration of resveratrol used, the entrapment efficiency of the drug decreases as would be expected, however the statistical analysis showed that the resveratrol concentration used, in the preparation of the formulations had no significant effect on the percentage of entrapment obtained ($P > 0.05$).

In summary, this type of solid lipid nanoparticles prepared with the optimized parameters could be considered suitable systems for resveratrol incorporation because it has high rates of encapsulation.

Particle size measurements

The mean particle sizes of the SLNs measured by DLS are presented in Table III. Both unloaded and resveratrol-loaded nanoparticles showed a homogenous size distribution with a mean diameter of about 150 nm and no statistically significant differences were observed ($P > 0.05$) between them, suggesting that resveratrol incorporation does not influence the nanoparticles size. Furthermore, it is important to note that the size of nanoparticles determined by DLS is carried out in aqueous state meaning that the lipid nanospheres are highly hydrated and because of that the diameters detected by this technique are usually larger than the non-hydrated diameters. Therefore the particles size obtained by DLS is in agreement with the results obtained by TEM, with slightly smaller sizes observed using the microscopic technique. TEM gives us an overview of all populations of nanoparticles as well as their diameters while the DLS, give us an average size of all sub populations.

Table III– Characterization of resveratrol-loaded SLNs. All values represent the mean \pm SD (n=3). No statistically significant differences were observed between any of the nanoparticle formulations ($p > 0.05$).

	Z-average (nm)	Polydispersity Index	Zeta Potential (mV)	Entrapment Efficiency (%)
SLN Placebo	151.2 \pm 12.0	0.191 \pm 0.060	-12.5 \pm 2.8	-
SLN RSV 2mg	157.4 \pm 14.9	0.142 \pm 0.032	-13.0 \pm 0.9	95.6 \pm 4.0
SLN RSV 5mg	151.5 \pm 5.8	0.161 \pm 0.065	-12.4 \pm 4.6	88.7 \pm 4.6
SLN RSV 10mg	162.1 \pm 6.8	0.124 \pm 0.061	-12.1 \pm 1.3	83.2 \pm 1.7
SLN RSV 15mg	174.0 \pm 5.0	0.108 \pm 0.040	-12.4 \pm 0.5	67.5 \pm 10.0

Meanwhile, PI values obtained were lower than 0.2 for all nanoformulations (Table III), suggesting that the nanoparticles were in a state of acceptable monodispersity distribution, with low variability and no aggregation. In fact, this type of distribution is usual in lipid nanoparticles made using the high shear homogenization and ultrasound method and is very difficult to achieve a unimodal distribution of sizes.^[2]

The mean diameters confirmed that the kind of lipid nanoparticles produced are submicron colloidal carriers, suitable for reach and cross the BBB as intended, because they have a reduced diameter with lower PI, showing that the optimization of the nanoparticles was successful.

Zeta potential measurements

As previously described the magnitude of the zeta potential gives an indication of the potential stability of the colloidal system. If all the particles have a very negative or very positive charge they will repel each other and therefore the dispersion will have a good stability. If particles have a low zeta potential, there will be agglomeration and instability in the dispersion. In general, particles can be considered stably dispersed when the absolute value of the zeta potential is above 30 mV due to the electric repulsion between the particles, while potentials between 5 mV and 15 mV result in limited flocculation and potentials between 0 mV and 5 mV yield a maximum flocculation.^[2]

As can be seen in table III all nanoformulations presented a negative average zeta potential of around -12 mV regardless of resveratrol incorporation, suggesting that resveratrol did not significantly change the zeta potential of the lipid nanoparticles ($P > 0.05$). Hence, the lipid nanoparticles that were developed in the present work may be considered physically stable due to the electrostatic repulsion conferred by the chemical nature of the lipid matrix, the polysorbate surfactant used, and possibly the adsorption of negatively charged ions onto the surface of the lipid nanoparticles. However it is necessary to do a stability study to improve the stability of this formulation over the time, since there may be some flocculation and aggregation once the zeta potential is not very high.

Release studies

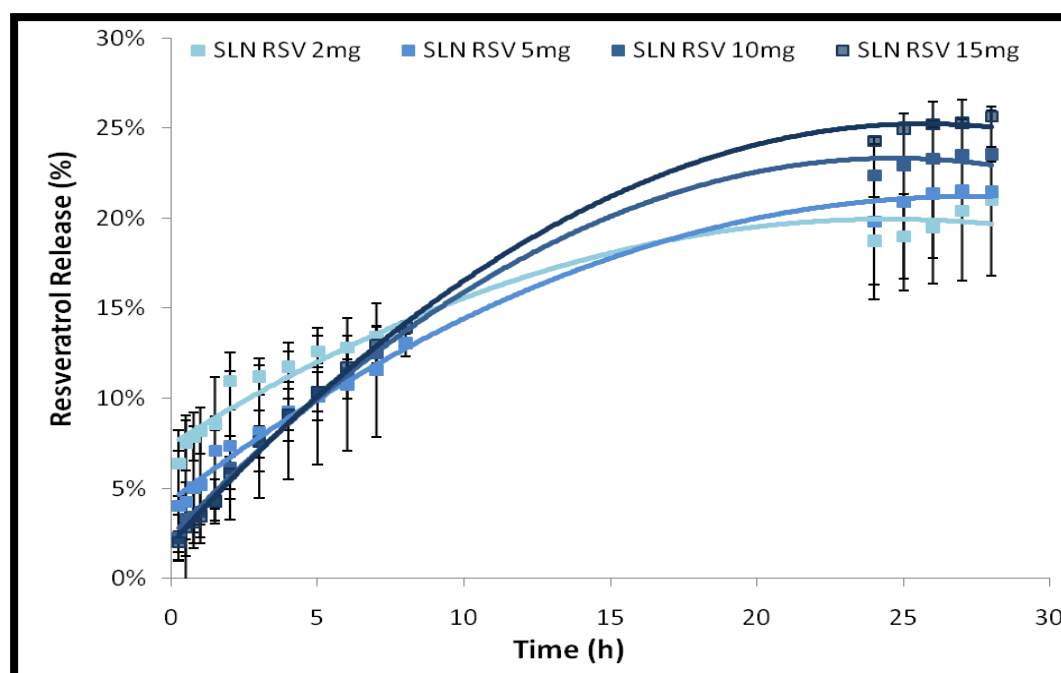


Figure 13 • *In vitro* resveratrol release profiles from resveratrol-loaded lipid nanoparticles with different concentrations of resveratrol, in SBF, simulating the blood stream conditions, at body temperature (37°C). All data represent the mean \pm SD ($n = 3$). No statistically significant differences were observed over the time for any resveratrol concentration ($P > 0.05$).

In vitro resveratrol release studies were performed in SBF (simulated body fluid) to simulate the blood stream conditions. In lipid nanoparticles the release of the drug loading is performed by diffusion of the drug from the inside of the particle or by degradation of the lipid matrix of SLNs.

Resveratrol is predominantly lipophilic, hence its tendency to localize at the core of the nanoparticle, but it also has three hydroxyl groups, which tend to localize at the interface near the shell, favoring the initial burst release within 5 hours that is shown in the figure 13 by the rapid release of resveratrol during the first 5 hours of assay.

In general, the statistical analysis showed that the resveratrol concentration used in the preparation of the formulations had no significant effect on the percentage of release ($P > 0.05$). SLNs had a resveratrol release almost residual for several hours

achieving a maximum release of 25%. This allows us to conclude that only residual amounts of resveratrol are released until SLNs reach their target, getting a large part of the encapsulated compound before crossing the BBB. In addition 28 hours after, the resveratrol release appears to reach a stationary phase providing possibly a more controlled and prolonged release of the encapsulated compound remaining.

Moreover, the degradation of the lipid matrix occurs mainly by lipases while only a small part is degraded by non-enzymatic hydrolytic processes. Another enzyme responsible for SLN degradation is the endogenous alcohol dehydrogenase. The tween 80 is a PEG-containing surfactants that provides a sterically protective layer of varying thickness depending on the structure and number of PEG units. The protective layer more or less hinders the lipid from the enzyme attack obstructing the anchorage of the lipase/colipase system. The lipid used in the synthesis of nanoparticles also influence the degradation rate, a higher degradation rate was observed for glyceride based SLN than for wax based SLN (e.g. cetyl palmitate). In fact waxes are not optimal substrates for lipase/colipase that preferentially metabolize glycerides.^[31] For all this reasons it is expectable that SLNs in the bloodstream does not release resveratrol prematurely.

Stability study

In order to evaluate the stability over time, each formulation was evaluated for average size, zeta potential and entrapment efficiency over 2 months (in the first week, after one month of storage and after two months of storage).

The physical stability of the lipid nanoparticles was evaluated firstly by examining changes of mean particle sizes during storage conditions that is shown in figure 14. For some formulations there are statistically significant differences ($P < 0.05$) particularly when comparing the average diameter after 2 months of storage with the initial average diameter, after the synthesis. For most of the formulations the average diameter increased after 2 months of storage. However this increase is slightly notorious what refutes the possibility of aggregation and agglomeration. Thus no aggregation is predicted for these formulations despite the slight increase in the

size which is not worrying from my point of view since the average diameter does not exceed 200 nm in most cases.

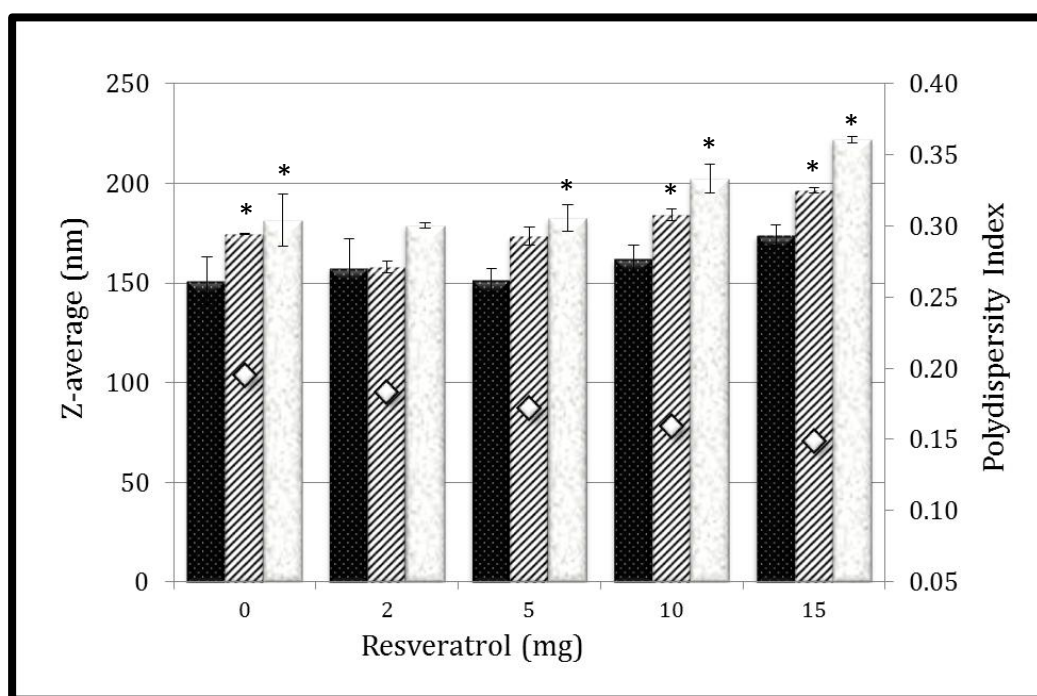


Figure 14 • Effect of time of storage (at 10°C) on particle size for SLNs at different concentrations of resveratrol. **Notes:** Z-average after 1 week (■), 1 month (▨), 2 months (▩), and PI (◇). All data represent the mean ± SD (n = 3). (*) denotes statistically significant differences ($P < 0.05$).

The physical stability of the lipid nanoparticles was also verified periodically by analyzing the variation of the zeta potential (figure 15). Zeta potential is a key factor in the evaluation of the stability of colloidal dispersions, since it is a function of the surface charge that gives the magnitude of the electrostatic repulsive interactions between particles. It is already shown earlier that the SLNs synthesized have a zeta potential of around -12 mV which could lead to some aggregation between particles. However with these results we conclude that the stability over time of SLNs synthesized is not compromised since no tendency for zeta potential to change was found during storage conditions for SLNs with and without resveratrol ($P > 0.05$).

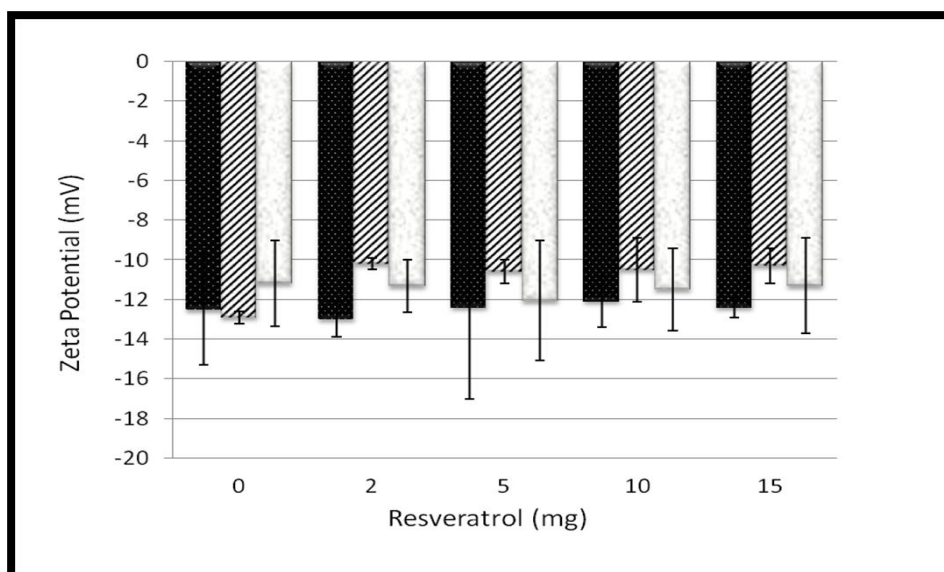


Figure 15 • Effect of time of storage (at 10°C) on zeta potential for SLNs at different concentrations of resveratrol. **Notes:** Z-average after 1 week (■), 1 month (▨) and 2 months (□). All data represent the mean \pm SD (n = 3). No statistically significant differences were observed over the time for any resveratrol concentration ($P > 0.05$).

Finally the physical stability of the lipid nanoparticles was also verified in terms of entrapment efficiency of resveratrol over the time. SLNs are characterized by having a highly organized matrix that tends to form perfect crystals over time which can eventually lead to an expulsion of the drug during the storage period. This is the main disadvantage of solid lipid nanoparticles hence the high interest in evaluating the quantity of resveratrol encapsulated over the time. Nevertheless as can be seen in figure 16 the entrapment efficiency hardly changed during the two months, with no significant differences between the amount of resveratrol encapsulated after synthesis and the amount of encapsulated resveratrol past two months. This suggests that SLNs retain the encapsulated compound over time precluding the possibility of expulsion of the drug, showing once again the stability of these formulations.

In general, this long-term stability study demonstrates that the optimization of SLNs done in this study resulted in a dynamic stable system capable of being used as controlled-release schemes for brain targeted resveratrol delivery, having an average size well below 200 nm. So the next step was the functionalization of the nanoparticles with ApoE to brain targeting.

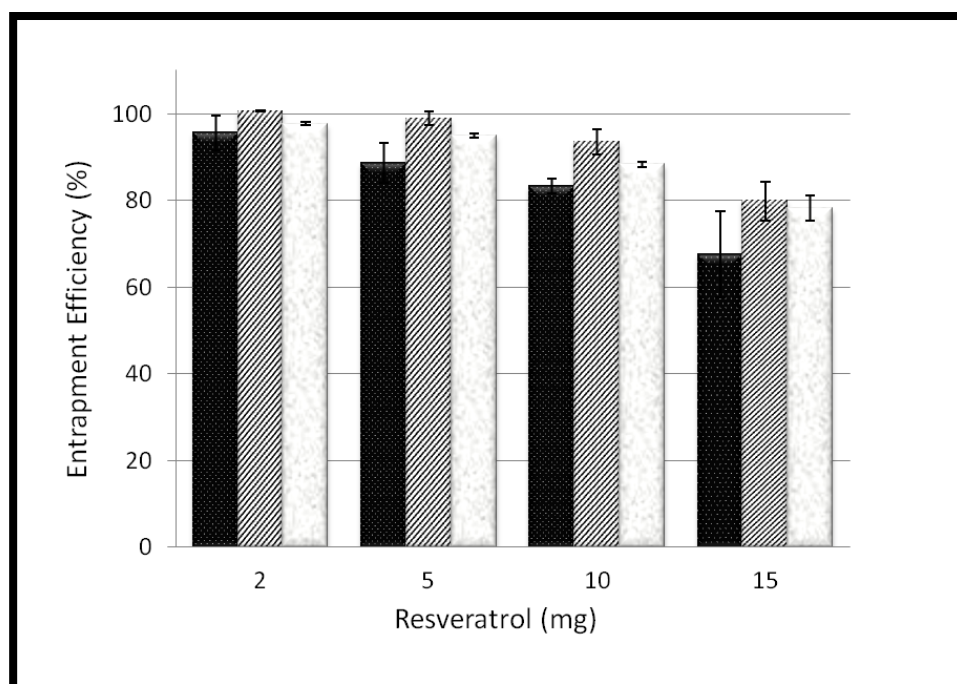


Figure 16 • Effect of time of storage (at 10°C) on resveratrol entrapment efficiency for SLNs at different concentrations of resveratrol. **Notes:** Z-average after 1 week (■), 1 month (▨) and 2 months (□). All data represent the mean \pm SD ($n = 3$). No statistically significant differences were observed over the time for any resveratrol concentration ($P > 0.05$).

SLNs Functionalized with ApoE

As already referred, the functionalization of solid lipid nanoparticles with ApoE was performed by two strategies: (i) using a phospholipid (DSPE-PEG-NH₂) to which avidin is added experimentally; and (ii) using palmitate with a terminal NHS that can also react with avidin. It was subsequently performed the characterization of each separately using the same parameters analyzed for the SLNs without functionalization: morphology, average size, PI, zeta potential and EE. The successful of functionalization was also confirmed by FTIR and fluorometric assays.

Strategy I: SLNs with DSPE-PEG-ApoE

In this case the particles are prepared incorporating DSPE-PEG-NH₂ in its composition. Subsequently, the avidin is conjugated to the nanoparticles by peptide bond between the amine terminal group of DSPE and the carboxyl group of avidin forming thereby nanoparticles conjugated with avidin. Finally the particles are added to previously biotinylated ApoE.

As in SLNs without functionalization, the functionalized SLNs morphology was analyzed by TEM. In figure 17 and 18 are shown the images recorded in the TEM concerning the ApoE functionalized SLNs with (SLN-DSPE-ApoE RSV) and without (SLN-DSPE-ApoE Placebo) resveratrol.

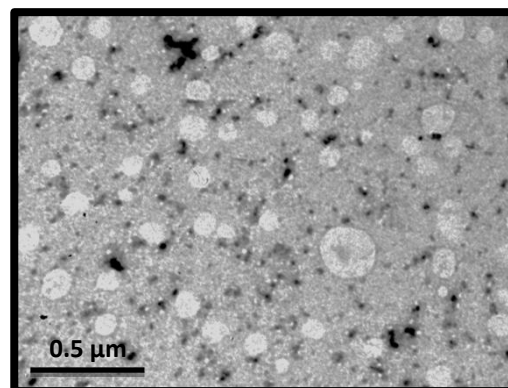


Figure 17 • TEM image of SLN-DSPE-ApoE Placebo.

As expected the SLNs functionalized have a spherical shape perfectly defined and is not visible aggregation and agglomeration of nanoparticles. Once again these formulations produce two populations of nanoparticles, one most abundant with a smaller diameter, and other, less pronounced, with a slightly large size. It is noted that, according to TEM images, the most abundant population has an average diameter less than 200 nm demonstrating again that the initial step of optimizing the size of the particles was successful.

In this case, resveratrol did not seem to cause morphological changes or crystal formation once resveratrol-loaded lipid nanoparticles have a shape similar to placebo nanoparticles and the diameter seems to be in the same scale.

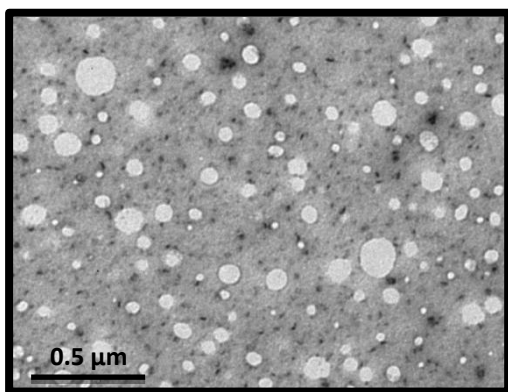


Figure 18 • TEM images of SLN-DSPE-ApoE RSV.

The results of average size, PI, zeta potential and entrapment efficiency are compiled in table IV. This table shows the characterization of SLNs without functionalization (to comparison), SLNs only with DSPE (SLN-DSPE-NH₂), SLNs with avidin linked to DSPE (SLN-DSPE-Avidin) and SLNs with ApoE that is linked to avidin (SLN-DSPE-ApoE).

As can be seen in table IV the average size and PI did not change significantly with the nanoparticle functionalization using DSPE. The zeta potential remained

unchanged in the functionalized particles (SLN-DSPE-ApoE), maintaining its potential in the order of -12 mV what is optimal to not compromise the stability of the particles. Concerning SLNsonly with DSPE-PEG-NH₂, the phospholipid has a terminal amine which at a pH of 7.4 is ionized, NH₃⁺, giving positive charge to the nanoparticles.

Table IV– Characterization of SLNs with ApoE using DSPE. All values represent the mean \pm SD (n=3). Results of SLNs without drug were analyzed and compared with SLN Placebo (no functionalization), and the results of SLNs with resveratrol were compared to SLN RSV (no functionalization). (*) denotes statistically significant differences (P < 0.05).

	Z-average (nm)	Polydispersity Index	Zeta Potential (mV)	Entrapment Efficiency (%)
SLN Placebo	151.2 \pm 12.0	0.191 \pm 0.060	-12.5 \pm 2.8	-
SLN RSV	151.5 \pm 5.8	0.161 \pm 0.065	-12.4 \pm 4.6	88.7 \pm 4.6
SLN-DSPE-NH ₂ Placebo	185.5 \pm 3.8	0.154 \pm 0.023	12.08 \pm 0.88 *	-
SLN-DSPE-NH ₂ RSV	178.3 \pm 15.8	0.187 \pm 0.023	10.64 \pm 0.93 *	93.2 \pm 5.7
SLN-DSPE-Avidin Placebo	168.9 \pm 41.2	0.167 \pm 0.087	-9.93 \pm 2.67	-
SLN-DSPE-Avidin RSV	167.5 \pm 40.2	0.183 \pm 0.098	-9.79 \pm 2.41	94.6 \pm 6.7
SLN-DSPE-ApoE Placebo	167.2 \pm 26.7	0.157 \pm 0.058	-10.86 \pm 1.68	-
SLN-DSPE-ApoE RSV	167.8 \pm 19.9	0.195 \pm 0.049	-13.05 \pm 4.06	98.0 \pm 2.5

In terms of entrapment efficiency the functionalization did not change the high rate of encapsulation of resveratrol already obtained for this type of nanoparticles since no significant differences were recorded at the level of entrapment efficiency between particles with and without functionalization (p > 0.05).

The nanoparticles have an average size less than 170 nm, with a good polydispersity (< 0.2), a zeta potential reasonably high to not allow clustering (~ -12 mV) and resveratrol entrapment efficiency very high (~ 90%). Thus we can conclude that the functionalization of the SLNs with ApoE using DSPE-PEG-NH₂ is a very promising technique that originates nanoparticles theoretically capable of reaching the BBB and go through it to reach the brain where resveratrol may exert its beneficial therapeutic effects.

Strategy II: SLNs with Palmitate-ApoE

In this case the process started with an avidin palmitoylation resulting in the formation of avidin palmitate which is then added to the lipid phase during the synthesis of SLNs. ApoE previously biotinylated is thereafter linked to the SLNs by avidin-biotin binding. Then the nanoparticles were characterized regarding morphology, average size, zeta potential and entrapment efficiency.

As for the other formulations, the SLN-Palmitate-ApoE morphology was analyzed by TEM. In figure 19 and 20 are shown the images recorded in the TEM without and with resveratrol, respectively.

As can be seen in figure 19 SLNs functionalized with ApoE using palmitate appears to be spherical with smooth surfaces in the case of SLNs placebo.

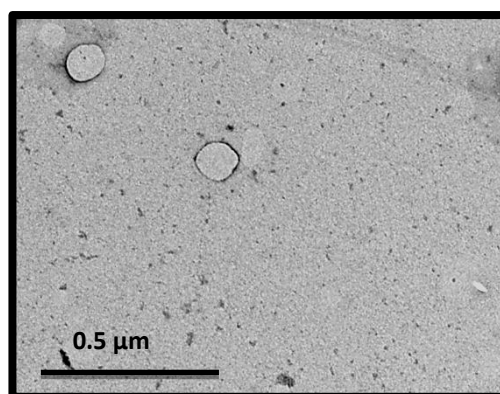


Figure 19 • TEM images of SLN-Palmitate-ApoE Placebo.

Resveratrol-loaded ones (figure 20) are also spherical but seem to have a wrinkled surface maybe because the resveratrol content inside the nanoparticles. In general, the diameter of these

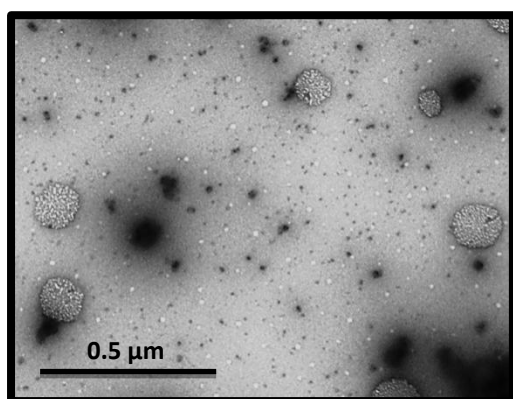


Figure 20 • TEM images of SLN-Palmitate-ApoE RSV.

functionalized nanosystems and placebo nanoparticles seems to be in the same scale. However, SLNs functionalized using palmitate seem to have an average size superior to SLNs functionalized using DSPE, but we can only draw assertive conclusions after analyze the average hydrodynamic size of the particles obtained by DLS.

The results of average size, PI, zeta potential and entrapment efficiency for this type of functionalization are summarized in table V. This table shows the characterization of SLNs without functionalization (to comparison), SLNs with avidin

palmitate(SLN-Palmitate-Avidin) and SLNs with ApoE that is linked to avidin (SLN-Palmitate-ApoE).

In this case significant differences were observed in the average size of SLNs functionalized in comparison with the reference nanoparticles (without functionalization), as would be expected by the images obtained from TEM. The average size round the 200 nm, but the population is more homogeneous because PI is lower when compared to particles without functionalization. One interesting fact is that resveratrol-loadedfunctionalized SLNs have a higher average size than the non-loadedfunctionalized SLNs which is explicable by the presence of resveratrol molecule inside the nanoparticles. At the same time they have a lower PI suggesting almost an unimodal dispersion which can be quite useful.

Regarding zeta potential the functionalization did not change this parameter, even though there is a slight increase in the negative zeta potential of the NPs. There were no significant differences in rates of drug encapsulation suggesting that the functionalization and the entire protocol for the addition of ApoE to NPs do not promote the expulsion of the drug. In reality with functionalization we can increase the entrapment efficiency to nearly 100%, however, it is very important to conduct a study of the stability of the NPs along time to check if the drug is not prematurely loss.

Table V– Characterization of SLNs with ApoE using palmitate. All values represent the mean \pm SD (n=3). Results of SLNs without drug were analyzed and compared with SLN Placebo (no functionalization), and the results of SLNs with resveratrol were compared to SLN RSV (no functionalization). (*) denotes statistically significant differences ($P < 0.05$).

	Z-average (nm)	Polydispersity Index	Zeta Potential (mV)	Entrapment Efficiency (%)
SLN Placebo	151.2 \pm 12.0	0.191 \pm 0.060	-12.5 \pm 2.8	-
SLN RSV	151.5 \pm 5.8	0.161 \pm 0.065	-12.4 \pm 4.6	88.7 \pm 4.6
SLN-Palmitate-Avidin Placebo	195.0 \pm 15.1 *	0.141 \pm 0.037	-12.22 \pm 0.29	-
SLN-Palmitate-Avidin RSV	207.1 \pm 3.7 *	0.073 \pm 0.018	-15.06 \pm 2.97	95.3 \pm 2.0
SLN-Palmitate-ApoE Placebo	192.3 \pm 13.1 *	0.136 \pm 0.112	-14.64 \pm 1.14 *	-
SLN-Palmitate-ApoE RSV	217.1 \pm 5.8 *	0.077 \pm 0.030	-13.54 \pm 1.60	98.9 \pm 0.6

This nanoparticles have an average size of around 200 nm, with a very good polydispersity (< 0.15), a zeta potential reasonably high (~ -15 mV) to not allow clustering and resveratrol entrapment efficiency very high ($\sim 90\%$). Thereby it is possible to say that the functionalization of the SLNs with ApoE using the avidin palmitate can also be a very promising technique that can be used to resveratrol delivery to BBB.

Release study with functionalized nanoparticles

For both types of functionalization, the resveratrol release assays were performed to verify if the addition of ApoE affected the controlled release of the drug. *In vitro* resveratrol release studies were performed in SBF to simulate the blood stream conditions, as previously described. This *in vitro* release study is a very important tool which is mainly useful for quality control as well as for the prediction of *in vivo* kinetics. The results can be seen in figure 21.

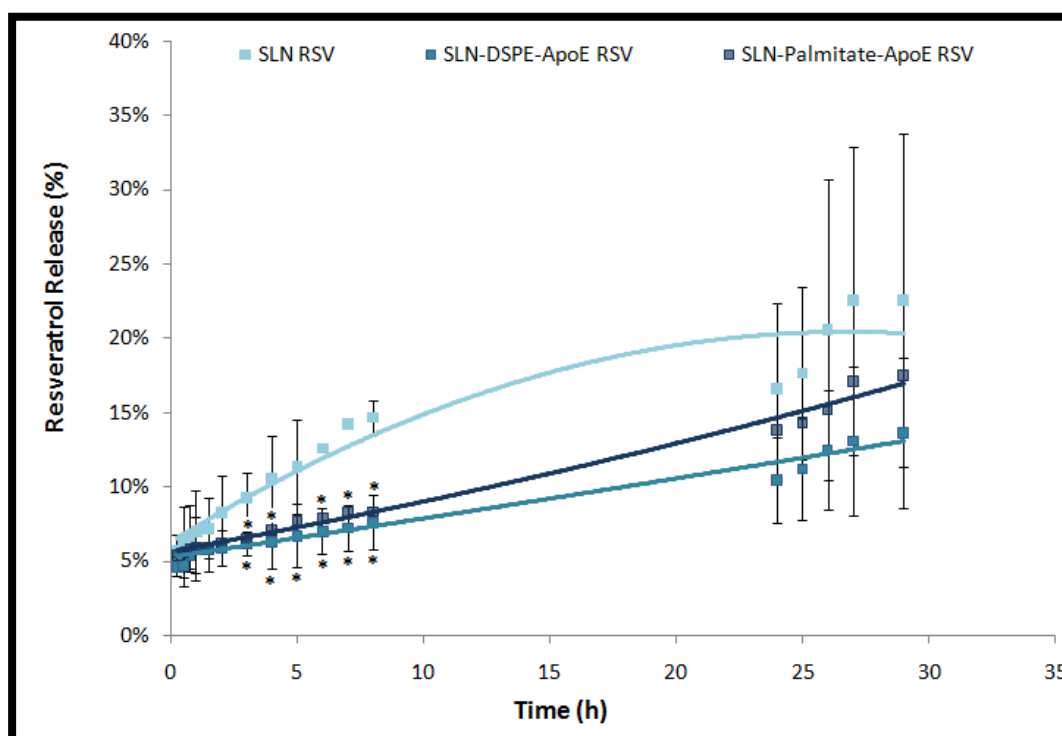


Figure 21 • *In vitro* resveratrol release profiles from non-functionalized SLNs and functionalized SLNs (SLN-DSPE-ApoE RSV and SLN-Palmitate-ApoE RSV), in SBF, simulating the blood stream conditions, at body temperature (37°C). All data represent the mean \pm SD ($n = 3$). (*) denotes statistically significant differences in relation to SLN RSV with no functionalization ($P < 0.05$).

Analyzing the results obtained we can conclude that there were no statistically significant differences in drug release with the nanoparticle functionalization. Moreover, it has been registered a more controlled resveratrol release, almost linear, from the functionalized SLNs in both functionalization strategies. The initial burst release during the first 5 hours is not as pronounced as it was in non-functionalized SLNs. In general, the drug release is made in a more gradual way after the addition of ApoE. Therefore, it is possible to infer that the functionalization does not compromise the sustained release of resveratrol in the blood stream.

Stability study of functionalized nanoparticles

After the characterization and the evaluation of drug release it is preponderant to evaluate if the stability of SLNs changed with the addition of ApoE. In this case due to the lack of time, the stability study for functionalized NPs could only be performed for 1 month. Each formulation was evaluated for average size, zeta potential and

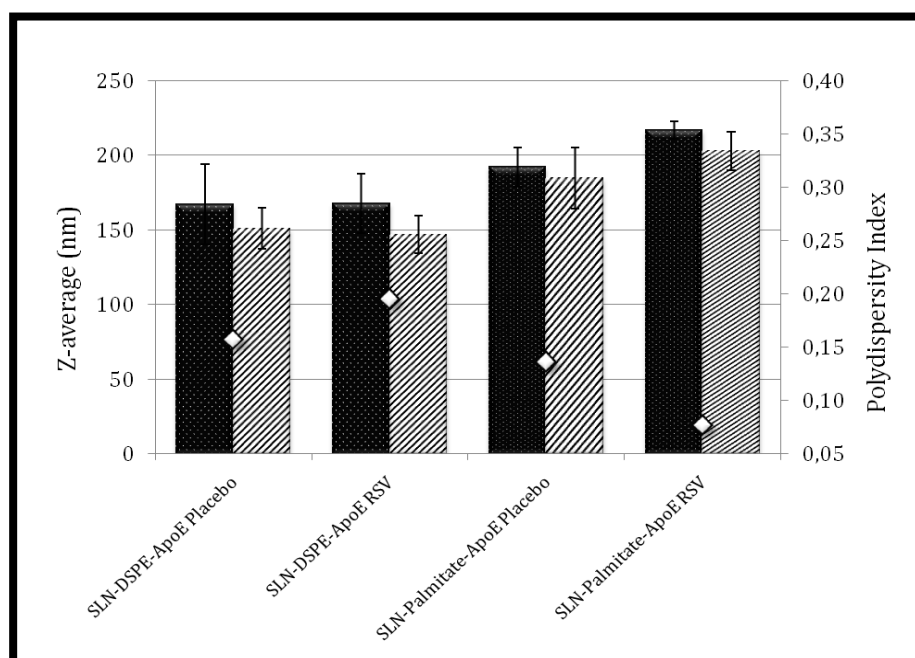


Figure 22 • Effect of time of storage (at 10°C) on particle size of ApoE functionalized SLNs. **Notes:** Z-average after 1 week (■), 1 month (▨) and PI (◇). All data represent the mean \pm SD ($n = 3$). No statistically significant differences were observed over time for any formulation ($P > 0.05$).

entrapment efficiency in the first week and after one month of storage.

In figure 22 is possible to see the results of the variation in average particle size over time. As can be seen size does not change significantly over time indicating that there are no aggregation of particles ($p > 0.05$) and that they are stable in solution after 1 month. Therefore, the ApoE functionalization of SLNs using DSPE or palmitate, originate stable formulations which do not form clusters during at least the first one month.

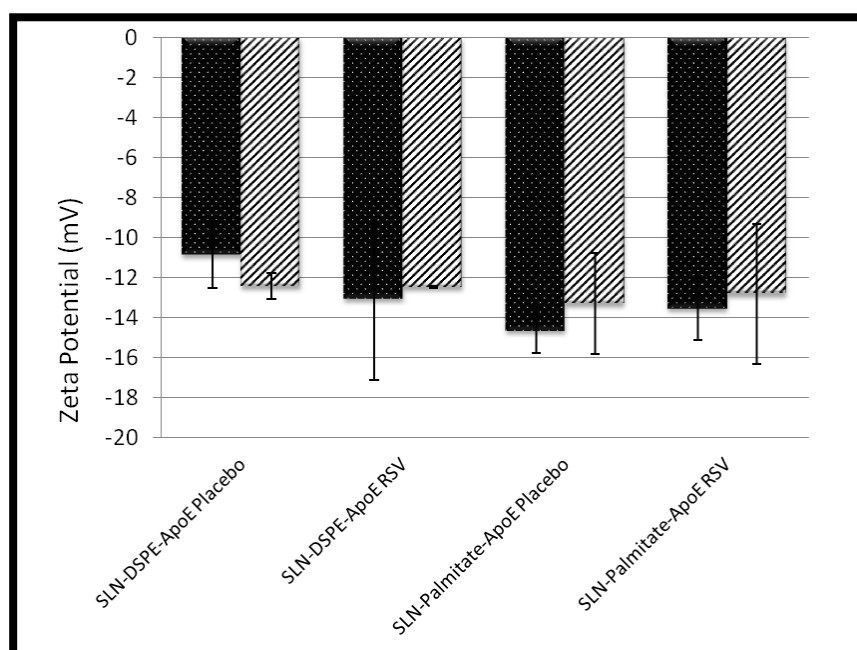


Figure 23 • Effect of time of storage (at 10°C) on zeta potential of ApoE functionalized SLNs. **Notes:** Z-average after 1 week (■) and 1 month (▨). All data represent the mean \pm SD ($n = 3$). No statistically significant differences were observed over time for any formulation ($P > 0.05$).

In relation to the zeta potential the addition of ApoE to the SLNs did not significantly alter the charge on the surface of the particles over time. After one month of storage no significant changes in the zeta potential of NPs functionalized can be seen in figure 23, what is fundamental to good stability of NPs in solution. Finally the physical stability of the lipid nanoparticles was also verified in terms of entrapment efficiency of resveratrol over the time (figure 24). Regarding the drug encapsulation rate, the quantity of encapsulated drug does not change significantly after one month of storage for SLNs functionalized with ApoE remaining above 90%.

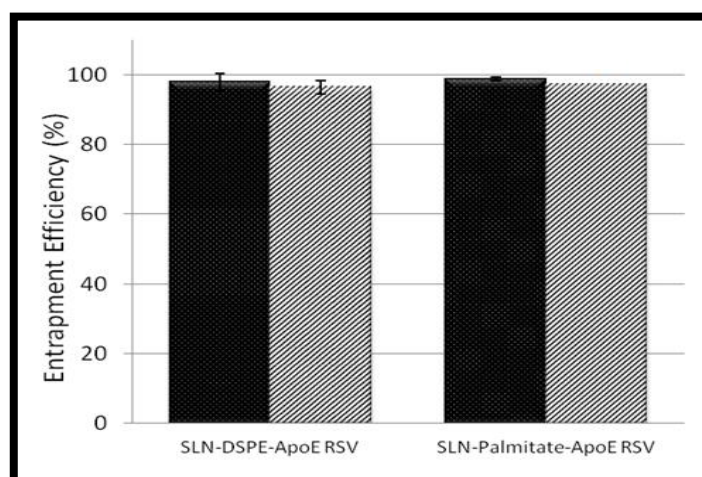


Figure 24 • Effect of time of storage (at 10°C) on resveratrol entrapment efficiency of ApoE functionalized SLNs. **Notes:** Z-average after 1 week (■) and 1 month (▨). All data represent the mean \pm SD ($n = 3$). No statistically significant differences were observed ($P > 0.05$).

In short, this long-term stability study demonstrates that the functionalization of SLNs with ApoE resulted in a dynamic stable system capable of being used as controlled-release schemes for targeting brain delivery of resveratrol by crossing the BBB via LDL receptor with average sizes in the order of 150 to 200 nm. No changes in mean particle sizes and zeta potential during storage conditions for 1 month have been reported. The entrapment efficiency remained very good with percentages of encapsulation over 90% indicating that there is no loss of resveratrol during storage.

FTIR

To prove that the functionalization was successful and that the ApoE is in fact linked to SLNs we had collected infra-red spectra for each lyophilized sample using

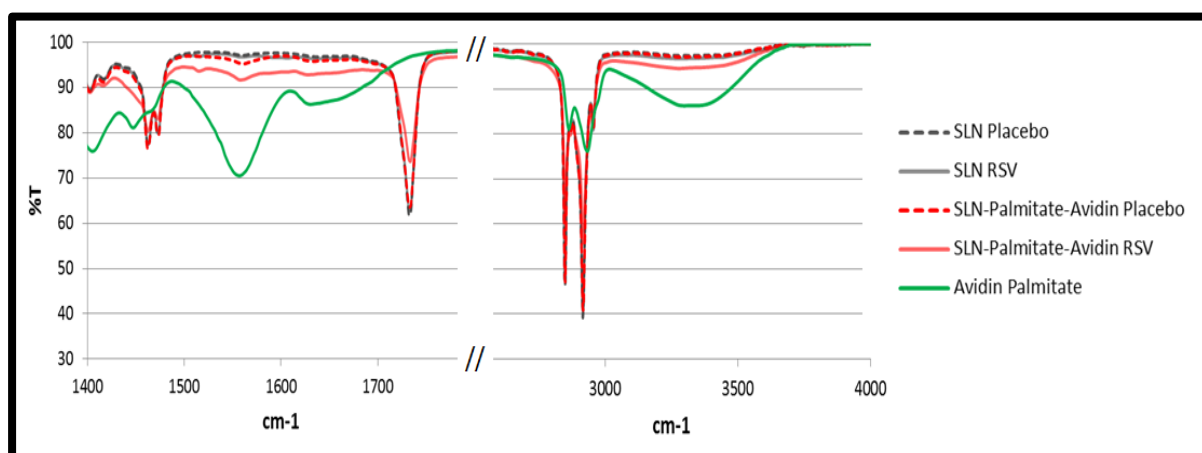


Figure 25 • Infrared spectrum obtained by FTIR for SLNs with no functionalization (SLN Placebo and SLN RSV); SLNs with avidin palmitate (SLN-Palmitate-Avidin Placebo and RSV) and avidin palmitate as a reference to compare with the functionalized samples.

FTIR. This makes possible to identify functional groups that lead to the detection and identification of avidin and ApoE in the formulations. A preliminary result consisted in demonstrate the presence of avidin in the particles for subsequent functionalization with ApoE. As can be seen in figure 25 there were two main peaks that stand out and demonstrate the presence of avidin. These two peaks match both to the NH groups that exist in the peptide bonds between aminoacids that form avidin. For particles not functionalized there are no NH groups so their presence comproves the presence of avidin linked to nanoparticles. There are one peak at $\sim 1550 \text{ cm}^{-1}$ that corresponds to bending vibrations of NH and other peak at $\sim 3400 \text{ cm}^{-1}$ (not so evident) that corresponds to stretch vibrations of the same group.

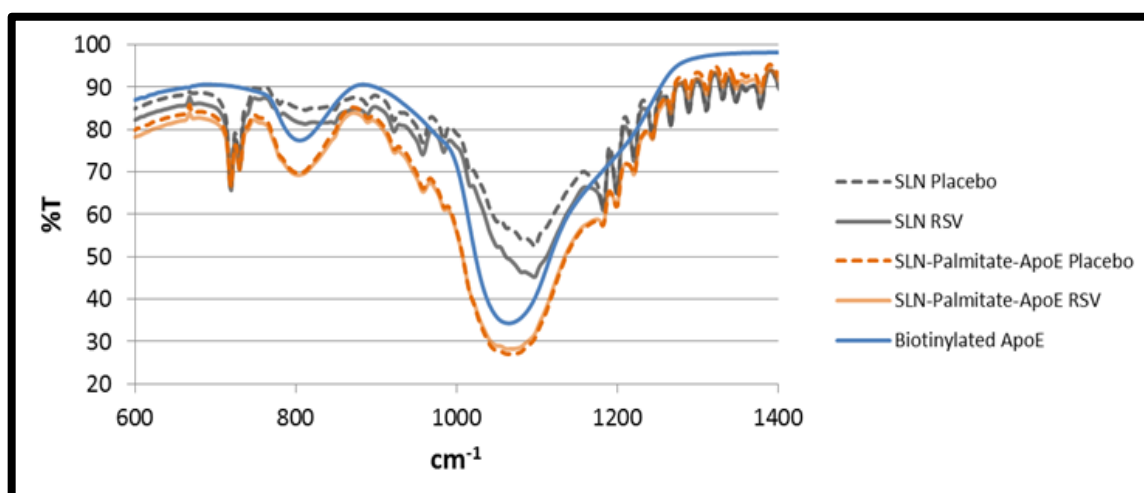


Figure 26 • Infrared spectrum obtained by FTIR for SLNs with no functionalization (SLN Placebo and SLN RSV); SLNs with ApoE (SLN-Palmitate-ApoE Placebo and RSV) and biotinylated ApoE as a reference to compare with the functionalized samples.

In figures 26 and 28 it is possible to confirm the presence of ApoE. In both types of functionalization are present two quite evident peaks which are not present in non-functionalized SLNs. One of them at $\sim 800 \text{ cm}^{-1}$ that corresponds to C-S bonds only present in biotin (see figure 28). The other peak at $\sim 1050 \text{ cm}^{-1}$ represents C-N bonds that are greatly increased in the presence of biotin (although there are also in avidin). Thus it is shown the presence of ApoE in

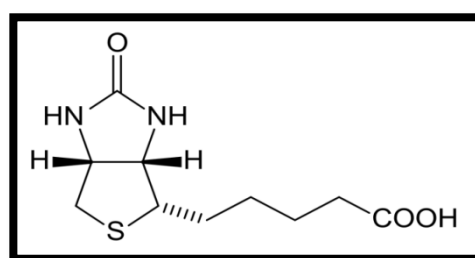


Figure 27 • Biotin Structure.

functionalized NPs once ApoE is biotinylated prior to addition to the particles (with the excess of biotin that did not bind removed by dialysis) and the presence of biotin is quite evident from the results of FTIR.

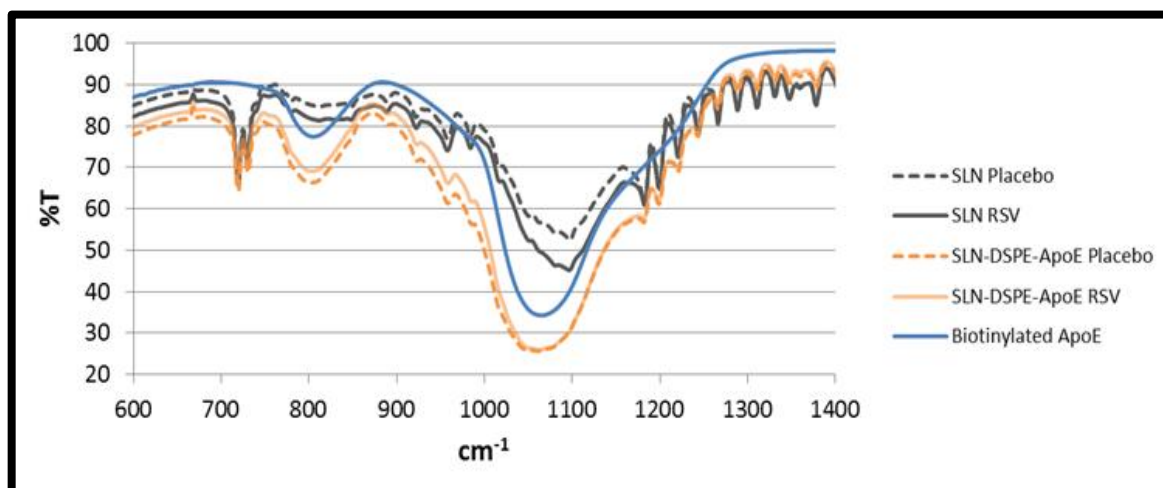


Figure 28 • Infrared spectrum obtained by FTIR for SLNs with no functionalization (SLN Placebo and SLN RSV); SLNs with ApoE (SLN-DSPE-ApoE Placebo and RSV) and biotinylated ApoE as a reference to compare with the functionalized samples.

Fluorometric assay

In addition to the infrared spectra, fluorometric assays were also performed to confirm the functionalization of the nanoparticles using a fluorescein biotin. This probe was used to quantify available biotin-binding sites on avidin. As already mentioned in

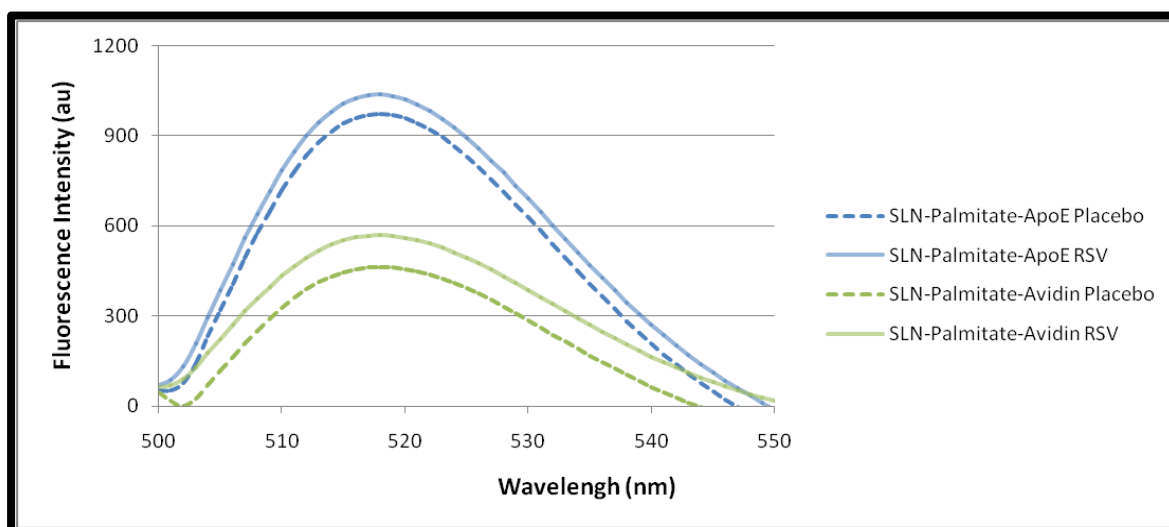


Figure 29 • Fluorometric assay using fluorescein biotin to comprove the presence of ApoE in the samples functionalized using palmitate. Blue lines represent formulations with ApoE and green lines represent formulations with only avidin (without ApoE linked).

materials and methods section there is a strong quenching phenomenon (the fluorescence intensity decreases) when the fluorescein binds to the free avidin sites on the surface of the NPs. So, if the functionalization is successful there will be little or no binding sites for the probe which will result in a maximum fluorescence of the fluorescein that is mostly in solution and thus expresses its fluorescence. Therefore the probe was incubated with the samples functionalized with ApoE and samples with avidin alone (without binding ApoE) for comparing the fluorescence obtained. Of course, when we have formulations only with avidin, there will be many sites for binding of fluorescein biotin resulting in a very sharp decrease in probe fluorescence. Figure 29 and 30 illustrates the results of fluorometric assays for SLNs functionalized with ApoE using palmitate and DSPE, respectively. As can be seen, there is a more pronounced fluorescence for SLNs with ApoE due to the lack of binding sites to the probe that are occupied by the presence of biotinylated ApoE. In both cases, there is an increase of fluorescence when compared SLNs only with avidin with SLNs with ApoE proving the presence of ApoE in the functionalized NPs.

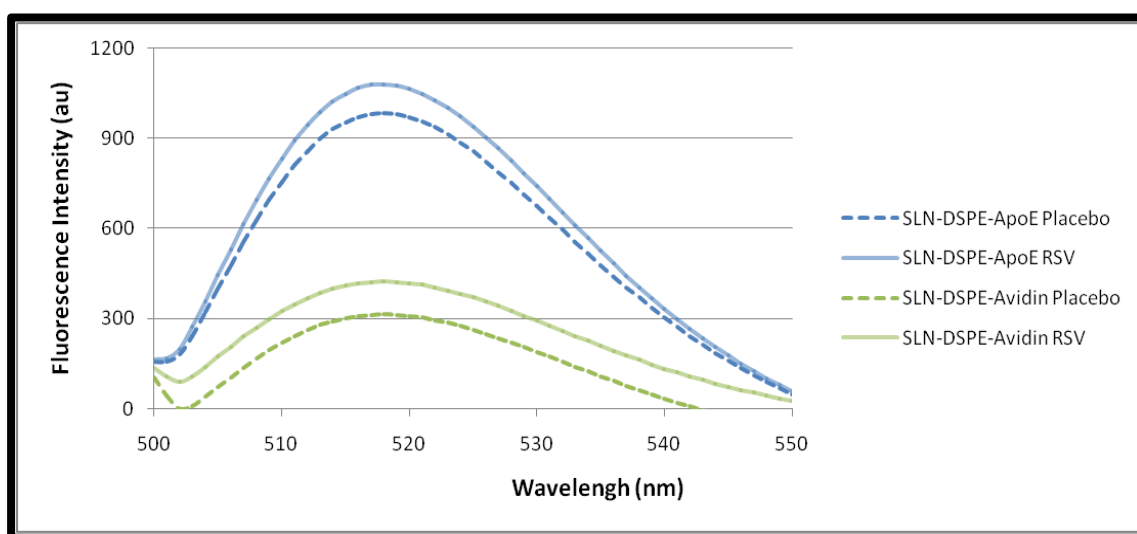


Figure 30 • Fluorometric assay using fluorescein biotin to comprove the presence of ApoE in the samples functionalized using DSPE. Blue lines represent formulations with ApoE and green lines represent formulations with only avidin (without ApoE linked).

Conclusion

The amazing growth in recent years of CNS study has generated enormous research efforts in an attempt to develop new drugs for brain diseases. However there are a low number of drugs entering the market what reflects the complexity of the CNS, certainly in great part due to the difficulty of crossing the BBB and reach the brain. Essentially 100% of large drugs and >98% of small drugs do not cross the BBB. Here the nanotechnology can be an important tool to improve the affinity of some drugs to the BBB, allowing them to be able to reach and cross this barrier and reach the brain.

The aim of this work is to take advantage of the neuroprotective effects of resveratrol. However when the compound is administered in its free form, little or no drug reach the brain due to its low bioavailability, low water solubility, and its chemical instability which causes a rapidly and extensively metabolism and excretion.

SLN delivery can be a promising way to administer drugs into the brain possibly overcoming the problems of solubility, permeability and toxicity associated with the administration of the free drug. It has been previously described that lipid NPs represent, in fact, promising carriers since their prevalence over other formulations in terms of toxicity, high stability, production feasibility and scalability.

In this study we developed a system capable of transport resveratrol, drive it to the brain facilitating its passage through the BBB, and allowing its sustained release over time by adding ApoE to SLN formulations. ApoE-functionalized SLNs may mimic lipoprotein particles that are endocytosed into the BBB endothelium and transcytosed through the BBB endothelium to the brain.

It was possible to successfully accomplish all the goals initially proposed. The optimization of SLNs done in this study resulted in dynamic stable systems capable of being used as controlled-release schemes for targeting brain delivery of resveratrol, having an average size well below 200 nm a reasonably negative zeta potential ($\sim -15\text{mV}$) and high rates of encapsulation of resveratrol (over 90%). Functionalization

of SLNs with ApoE was clearly demonstrated through fluorometric assays and the infrared spectra (using FTIR) for both types of functionalization performed. The functionalization of the SLNs with ApoE using DSPE or palmitate is a very promising technique that originates nanoparticles theoretically capable of reaching the BBB and go through it to reach the brain where resveratrol may exert its beneficial therapeutic.

This addition of ApoE to the formulations did not change significantly the long-term stability of the formulations already evaluated previously (for SLNs without ApoE). In fact for functionalized NPs, no changes in mean particle sizes and zeta potential during storage conditions for 1 month have been reported and the entrapment efficiency remained very good, indicating that there are no losses of resveratrol during storage.

Regarding the release of resveratrol there was no statistical significant differences after adding ApoE to SLNs suggesting that the functionalization does not compromise the sustained release of the drug.

This new approach of SLNs functionalization with ApoE had never been described before and it was quite successful developed.

Future work

Only in future it will be possible to say what type of functionalization is the best and the most profitable in therapeutic terms. Now it is necessary to show the effectiveness of each system in the improving of SLNs uptake into the brain. Therefore, it will of great importance to show and verify the advantages and effectiveness of these innovative SLNs formulations functionalized with ApoE through cellular studies *in vitro*. These studies will be done in hCMEC/D3 cell line showed in figure 31 that corresponds to immortalized human cerebral microvascular endothelial cells used as a model of human BBB.

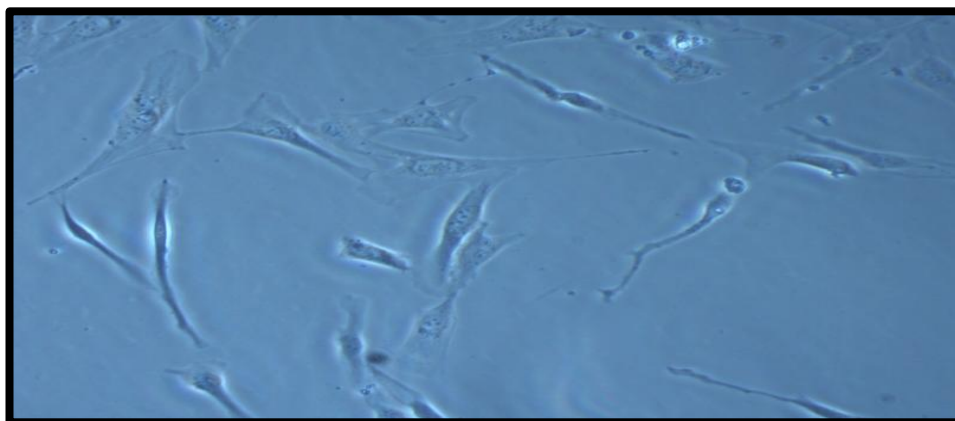


Figure 31 • Microscope image of hCMEC/D3 cell line.

In hCMEC/D3 cell line it will be done studies of cell viability and integrity by MTT assay and LDH test. It will also be held permeability studies in *Transwell*® permeable supports to assess whether in fact the functionalization of nanoparticles facilitates their passage through BBB. In addition is necessary to check if the functionalization induces an increased uptake of the NPs into the cells doing internalization studies using fluorescence microscopy and or flow cytometry.

Bibliography

- [1] Neves, A.; Lúcio, M.; Lima, J.L.F.C. and Reis, S.; Resveratrol in Medicinal Chemistry: A Critical Review of its Pharmacokinetics, Drug-Delivery, and Membrane Interactions; *Curr. Med. Chem.***2012**, 19, 1663-1681.
- [2] Neves, A.; Martins, S.; Lúcio, M.; Lima, J.L.F.C. and Reis, S.; Novel resveratrol nanodelivery systems based on lipid nanoparticles to enhance its oral bioavailability; *International Journal of Nanomedicine*. **2013**, 8, 177–187.
- [3] Langcake, P.; Pryce, R. J. Production of resveratrol by *Vitis-vinifera* and other members of vitaceae as a response to infection or injury. *PhysiologicalPlantPathology*.**1976**, 9(1), 77-86.
- [4] Soleas, G. J.; Diamandis, E. P.; Goldberg, D. M. Resveratrol: A molecule whose time has come? And gone? *Clin. Biochem.***1997**, 30(2), 91-113.
- [5] Douillet-Breuil, A. C.; Jeandet, P.; Adrian, M.; Bessis, N. Changes in the phytoalexin content of various *Vitis* spp. in response to ultraviolet C elicitation. *J. Agric. Food Chem.***1999**, 47(10), 4456-4461.
- [6] Adrian, M.; Jeandet, P.; Douillet-Breuil, A. C.; Tesson, L.; Bessis, R. Stilbene content of mature *Vitisvinifera* berries in response to UV-C elicitation. *J. Agric. Food Chem.***2000**, 48(12), 6103-6105.
- [7] Schubert, R.; Fischer, R.; Hain, R.; Schreier, P. H.; Bahnweg, G.; Ernst, D.; Sandermann, H. An ozone-responsive region of the grapevine resveratrol synthase promoter differs from the basal pathogen-responsive sequence. *Plant Mol.Biol.***1997**, 34(3), 417-426.
- [8] Adrian, M.; Jeandet, P.; Veneau, J.; Weston, L. A.; Bessis, R. Biological activity of resveratrol, a stilbenic compound from grapevines, against *Botrytis cinerea*, the causal agent for gray mold. *J. Chem. Ecol.***1997**, 23(7),1689-1702.

- [9] Bertelli, A. A. E.; Giovannini, L.; DeCaterina, R.; Bernini, W.; Migliori, M.; Fregoni, M.; Bavaresco, L.; Bertelli, A. Antiplatelet activity of cisresveratrol. *Drug Exp. Clin. Res.* **1996**, 22(2), 61-63.
- [10] Lekli, Diptarka Ray, Dipak K. Das Longevity nutrients resveratrol, wines and grapes Istvan, *Genes Nutr.* **2010**, 5, 55–60.
- [11] RE King, JA Bomser and DB Min. Bioactivity of Resveratrol, *Comprehensive Reviews in Food Science and Food Safety*. **2006**, 5, 65–70.
- [12] Sun AY, Simonyi A, Sun GY. The “French Paradox” and beyond: neuroprotective effects of polyphenols. *Free Radic Biol Med.* **2002**, 314–318.
- [13] Renaud S, Gueguen R. The French paradox and wine drinking. *Novartis Found Symp.* **1998**, 216, 208-17.
- [14] Das DK, Sato M, Ray PS, Maulik G, Engelman RM, Bertelli AA, Bertelli A Cardioprotection of red wine: role of polyphenolic antioxidants. *Drugs Exp Clin Res.* **1999**, 25, 115–120.
- [15] Bertelli, A. A. A.; Das, D. K. Grapes, Wines, Resveratrol, and Heart Health. *Journal of Cardiovascular Pharmacology*. **2009**, 54(6), 468-476.
- [16] Szkudelska, K.; Szkudelski, T. Resveratrol, obesity and diabetes. *Eur. J. Pharmacol.* **2010**, 635(1-3), 1-8.
- [17] Saiko, P.; Szakmary, A.; Jaeger, W.; Szekeres, T. Resveratrol and its analogs: Defense against cancer, coronary disease and neurodegenerative maladies or just a fad? *Mutat. Res.-Rev. Mutat. Res.* **2008**, 658(1-2), 68-94.
- [18] Marambaud, P.; Zhao, H. T.; Davies, P. Resveratrol promotes clearance of Alzheimer's disease amyloid-beta peptides. *J. Biol. Chem.*, **2005**, 280(45), 37377-37382
- [19] Feng Jin; Qin Wu; Yuan-Fu Lu; Qi-Hai Gong; Jing-Shan Shi. Neuroprotective effect of resveratrol on 6-OHDA-induced Parkinson's disease in rats. *European Journal of Pharmacology*, **2008**, 600 (1-3), 78-82.

- [20] Kwok-Tung Lu, Meng-Chang Ko et al. Neuroprotective Effects of Resveratrol on MPTP-Induced Neuron Loss Mediated by Free Radical Scavenging. *J. Agric. FoodChem.* **2008**, 56 (16), 6910–6913.
- [21] Rocha-González HI, Ambriz-Tututi M, Granados-Soto V. Resveratrol: a natural compound with pharmacological potential in neurodegenerative diseases. *CNS Neurosci Ther.* **2008**, 14(3), 234-47.
- [22] Walle T, Hsieh F, DeLegge MH, Oatis JE Jr, Walle UK. High absorption but very low bioavailability of oral resveratrol in humans. *Drug Metab Dispos.* **2004**, 32(12), 1377–1382.
- [23] Abbott NJ, Patabendige AA, Dolman DE, Yusof SR, Begley DJ. Structure and function of the blood-brain barrier. *Neurobiology of Disease.* **2010**, 37 (1), 13-25.
- [24] Yan Chen, Lihong Liu. Modern methods for delivery of drugs across the blood-brain barrier. *Advanced Drug Delivery Reviews.* **2012**, 64, 640-665.
- [25] Zensi A, Begley D, Pontikis C, Legros C, Mihoreanu L, Wagner S, Büchel C, von Briesen H, Kreuter J. Albumin nanoparticles targeted with Apo E enter the CNS by transcytosis and are delivered to neurones. *Journal of Controlled Release.* **2009**, 137, 78-86.
- [26] Kaur I., Bhandari R., Bhandari S., Kakkar V. Potential of solid lipid nanoparticles in brain targeting. *Journal of Controlled Release.* **2008**, 127, 97-109.
- [27] Wong H., Chattopadhyay N., Wu X., Bendayan R. Nanotechnology applications for improved delivery of antiretroviral drugs to the brain. *Advanced Drug Delivery Reviews.* **2010**, 62, 503-517.
- [28] Müller RH, Rühl D, Runge S, Schulze-Forster K, Mehnert W. Cytotoxicity of solid lipid nanoparticles as a function of the lipid matrix and the surfactant. *Pharm Res.* **1997**, 14(4), 458-62.

- [29] Chattopadhyay N, Zastre J, Wong HL, Wu XY, Bendayan R. Solid lipid nanoparticles enhance the delivery of the HIV protease inhibitor, atazanavir, by a human brain endothelial cell line. *Pharm Res.* **2008**,25(10), 2262-71.
- [30] David J. Begley. Delivery of therapeutic agents to the central nervous system: the problems and the possibilities. *Pharmacology & Therapeutics.* **2004**, 104, 29-45.
- [31] Blasi P., Giovagnoli S., Schoubben A., Ricci M., Rossi C. Solid lipid nanoparticles for targeted brain drug delivery. *Advanced Drug Delivery Reviews.* **2007**, 59, 454-477.
- [32] Torsten M., Goppert & Rainer H. Muller. Polysorbate-stabilized solid lipid nanoparticles as colloidal carriers for intravenous targeting of drugs to the brain: Comparison of plasma protein adsorption patterns. *Journal of Drug Targeting.* **2005**, 13(3), 179-187.
- [33] Wagner S., Zensi A., Wien S., Tschickardt S., Maier W., Vogel T., Worek F., Pietrzik C., Kreuter J., Hagen von Briesen. Uptake Mechanism of ApoE-Modified Nanoparticles on Brain Capillary Endothelial Cells as a Blood-Brain Barrier Model. *PLoS ONE.* **2012**, 7 (3), e32568
- [34] K. Michaelis, M. M. Hoffmann, S. Dreis, E. Herbert, R. N. Alyautdin, M. Michaelis, J. Kreuter, and K. Langer. Covalent Linkage of Apolipoprotein E to Albumin Nanoparticles Strongly Enhances Drug Transport into the Brain. *The Journal Of Pharmacology And Experimental Therapeutics.* **2006**, 317(3), 1246–1253.
- [35] Hoffmann M, Scharnagl H, Panagiotou E, Banghard W, Wieland H, März W. Diminished LDL receptor and high heparin binding of apolipoprotein E2 Sendai associated with lipoprotein glomerulopathy. *Journal of the American Society of Nephrology.* **2001**, 12(3), 524-30.
- [36] Triplett II, M.D., Enabling Solid Lipid Nanoparticle Drug Delivery Technology by Investigating Improved Production Techniques. **2004**, The Ohio State University: Ohio. p. 172.
- [37] Mehnert W, Mäder K. Solid lipid nanoparticles: production, characterization and applications. *Adv Drug Deliv Rev.* **2001**, 47 (2–3), 165–196.

- [38] Zetasizer Nano Series User Manual MAN0317. **2004**, Issue 2.1
- [39] T. Kokubo, H. Kushitani, S. Sakka, T. Kitsugi et T. Yamamuro; Solutions able to reproduce in vivo surface-structure changes in bioactive glass-ceramic A-W, *J. Biomed. Mater. Res.* **1990**, 24, 721-734.
- [40] A. Oyane, H. Kim, T. Furuya, T. Kokubo, T. Miyazaki et T. Nakamura; Preparation and assessment of revised simulated body fluids. *Wiley Periodicals, Inc. J Biomed Mater Res.* **2003**, 65A, 188-195.
- [41] Peter R. Griffiths, James A. de Haseth: Fourier transform infrared spectrometry (2nd edn.) *Analytical and Bioanalytical Chemistry*. **2008**, 391, 2379-2380.

Annex



Figure A.1 • Pictures of the SLNs synthesized during the optimization process.

Table AI • Visual characterization of the SLNs synthesized during the optimization process

	Milk Appearance	Granules	2 Phases	Air bubbles	Foam	Deposit Formation	Others
SLN 1	Yes	Very few	Yes - A very small stage in the background translucent	Very few	No	Small granules	It is possible to observe some sediment in the formulation tube wall
SLN 2	Yes	Very few and small	No	Very few	No	No	Looks good, very milky, with almost imperceptible granules
SLN 3	Yes	No	No	Very few	No	No	It is possible to observe some sediment in the tube wall of formulation, but the solution is apparently uniform
SLN 4	Yes	No	No	Very few	No	No	É possível observar vários sedimentos na parede do tubo de formulação
SLN 5	Yes	Very few	No	Very few	No	No	It is possible to observe various sediment in the formulation tube wall
SLN 6	A little bit	Some	No	Few	No	No	Some sediment cling to the wall and does not flow after shaking
SLN 7	A little bit	Some	No	Yes	No or very few	No (small sediments)	After shaking several small air bubbles and sediment does not flow and remain on the wall
SLN 8	A little bit	Yes (some big)	No	Very few	No	No	By shaking various sediments and large granules not trickle down and remain on the wall
SLN 9	A little bit	Yes	No	Yes	No	Yes (big)	It can be seen that large granules remain in the formulation tube wall even after agitation
SLN 10	Yes	Yes	No	No	No	No	It is possible to observe various sediment in the tube wall of formulation
SLN 11	Yes	Some	No	Yes	Very few	No	There are several sediment in the tube wall with irregular sizes
SLN 12	Yes	Yes	No	Yes	No	No	Is possible to see several large sediment in the formulation tube wall
SLN 13	No	Yes	Yes - A phase slightly translucent and other opaque and white in equal proportions	Yes	Yes	No	Some sediment cling to the wall and does not flow after shaking
SLN 14	Yes	No	No	No	No	No	Excellent aspect
SLN 15	Little	No	Yes - A huge translucent phase and a thin film on top opaque white	Yes	Yes	No	Almost solid layer on top phase
SLN 16	A little bit	No	Yes - A phase translucent very small on the basis and an extensive phase opaque white	Few	No	No	
SLN 17	A little bit	Very few	No	Very few	No	No	Some sediment cling to the wall and does not flow after shaking
SLN 18	No	Yes	Yes - A translucent phase and a phase opaque and white in equal proportion	Very few	No	Yes (sediments)	The granules remain on the wall after unrest
SLN 19	Very little	Yes	Yes - A phase translucent (small) and a phase opaque white (large)	No	No	Yes (sediments)	Some sediment cling to the wall and does not flow after shaking
SLN 20	A little bit	No	No	Few	No	No	Some sediment cling to the wall and does not flow after shaking
SLN 21	No	Yes	Yes - A phase translucent and other opaque white in equal proportion	Some	No	Yes (sediments)	This mixture does not appears homogeneous
SLN 22	Very little	No	Yes - A translucent phase and a minor white phase quite foamy	Yes	Yes (a lot)	Foam	It is possible to observe various sediment in the formulation tube
SLN 23	A little bit	Yes	Yes - A huge white opaque phase and a translucent phase much smaller	Yes	Few	No	There is a huge lipid aggregate on top of formulation
SLN 24	No	Yes	Yes - A phase almost translucent, which represents about 2/3 of the formulation, and a with opaque phase without foam	Some	Yes	Yes (sediments)	Various sediments are visible on the wall that does not flow after shaking
SLN 25	No	No	Yes - A large and translucent phase and a white and opaque phase much smaller with bubbles	Yes	Yes	No	Air bubbles remain in the walls without sagging after shaking
SLN 26	Little	No	Yes - Phases of equal size, one quite opaque and white and other translucent	Yes	No	No	Plenty of liquid
SLN 27	Little	Some	No	Yes	No	Yes	Curdled milk appearance, moves as an entire block
SLN 28	No	Yes	Yes - A large white and more solid phase and a translucent phase	Yes	Yes	No	It is possible to observe various sediment in the formulation tube wall